Island Arc

Island Arc (2016) **25**, 253–273

Research Article

Contributions of slab fluid and sediment melt components to magmatism in the Mariana Arc–Trough system: Evidence from geochemical compositions and Sr, Nd, and noble gas isotope systematics

YASUO IKEDA,[1,*,†] KEISUKE NAGAO,[2,‡] TERUAKI ISHII,[3,§] DAISUKE MATSUMOTO,[2] ROBERT J. STERN,[4] HIROO KAGAMI,[5,¶] MAKOTO ARIMA,[6] AND SHERMAN H. BLOOMER[7]

[1]*Department of Earth Science, Hokkaido University of Education, Kushiro, Hokkaido, Japan,* [2]*Geochemical Research Center, Graduate School of Science, University of Tokyo, Tokyo, Japan,* [3]*Ocean Research Institute, University of Tokyo, Nakano, Japan,* [4]*Geosciences Department, University of Texas at Dallas, Richardson, TX, USA,* [5]*Graduate School of Science and Technology, Niigata University, Niigata, Japan,* [6]*Graduate School of Environment and Information Sciences, Yokohama National University, Yokohama, Japan,* [7]*Department of Geoscience, Oregon State University, Corvallis, OR, USA*

Abstract This study presents new major and trace element, mineral, and Sr, Nd, and noble gas isotope geochemical analyses of basalts, gabbro, and clinopyroxenite from the Mariana Arc (Central Islands and Southern Seamount provinces) including the forearc, and the Mariana Trough (Central Graben and Spreading Ridge). Mantle source compositions beneath the Mariana Arc and the Mariana Trough indicate a mantle source that is depleted in high field strength elements relative to MORB (mid-oceanic ridge basalt). Samples from the Mariana Arc, characterized by high ratios of Ba/Th, U/Th, $^{84}Kr/^{4}He$ and $^{132}Xe/^{4}He$, are explained by addition of fluid from the subducted slab to the mantle wedge. Correlations of noble gas data, as well as large ion lithophile elements, indicate that heavy noble gases (Ar, Kr, and Xe) provide evidence for fluid fluxing into the mantle wedge. On the other hand, major elements and Sr, Nd, He, and Ne isotopic data of basalts from the Mariana Trough are geochemically indistinguishable from MORB. Correlations of $^{3}He/^{4}He$ and $^{40}Ar/^{36}Ar$ in the Mariana Trough samples are explained by mixing between MORB and atmosphere. One sample from the Central Graben indicates extreme enrichment in $^{20}Ne/^{22}Ne$ and $^{21}Ne/^{22}Ne$, suggesting incorporation of solar-type Ne in the magma source. Excess ^{129}Xe is also observed in this sample suggesting primordial noble gases in the mantle source. The Mariana Trough basalts indicate that both fluid and sediment components contributed to the basalts, with slab-derived fluids dominating beneath the Spreading Ridge, and that sediment melts, characterized by high La/Sm and relatively low U/Th and Zr/Nb, dominate in the source region of basalts from the Central Graben.

Key words: basalt, fluid, mantle source, Mariana Arc, Mariana Trough, noble gas isotopes, sediment, Sr–Nd isotopes.

INTRODUCTION

In subduction zones, subducted sediment, hydrated oceanic crust, and mantle lithosphere all interact with the overlying mantle wedge, causing chemical compositional and physical changes in the mantle wedge, and resulting in a heterogeneous source for island arc magmas. In addition, the Mariana Arc–Trough system records changing tectonic and melt generation processes that are

*Correspondence: Department of Earth Science Hokkaido University of Education at Kushiro, Kushiro 085-8580, Hokkaido, Japan (email: ikeda@zb.cyberhome.ne.jp).

†Current Address: Sagamihara-city, Kanagawa, Japan

‡Current Address: Korea Polar Research Institute, Yeonsu-gu, Incheon, Korea

§Current Address: Fukada Geological Institute, Tokyo, Japan

¶Current Address: Omachi, Nagano, Japan

Received 2 December 2014; accepted for publication 30 January 2016.

 doi:10.1111/iar.12150

typically associated with evolving back-arc basins, such as the Mariana Trough (e.g. Gribble *et al.* 1998; Kelley *et al.* 2010). The Mariana Arc is subdivided along strike into the Northern Seamount Province, the Central Island Province, and the Southern Seamount Province (Stern *et al.* 1988). The Mariana Trough backarc basin is also subdivided along strike. Martinez *et al.* (1995) divided the extensional axis of the Mariana Trough into four sections (see Fig. 1): (i) the northern volcano-tectonic zone (NVTZ, 23.1°N–22.1°N), characterized by asymmetric rifting; (ii) the southern volcano-tectonic zone (SVTZ, 22.1°N–21.0°N), characterized by southward-progressive separation of the extensional axis from the arc; (iii) the Central Graben (21°N–19.7°N), characterized by mechanical extension; and (iv) the Spreading Ridge (south of 19.7°N), where seafloor spreading takes place. Rifting-related lavas close to the NVTZ–SVTZ area that formed during the earliest stages of northern Mariana Trough evolution are indistinguishable from Mariana Arc lavas (Stern *et al.* 1990; Gribble *et al.* 1998). In comparison,

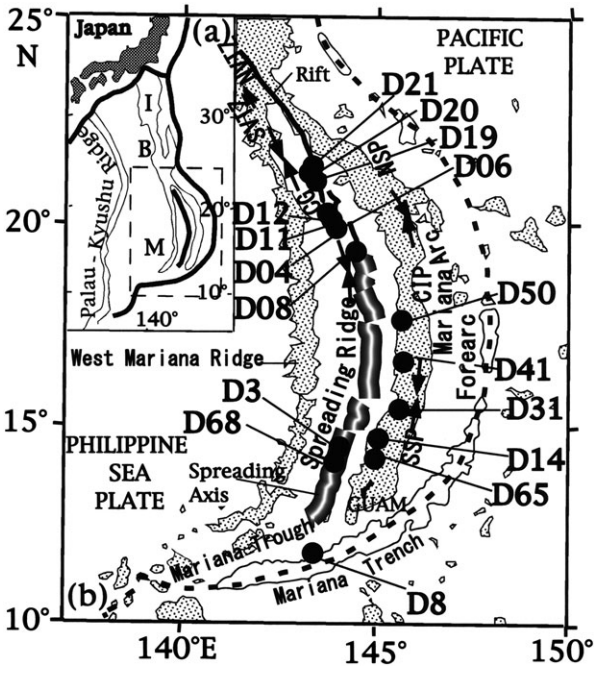

Fig. 1 (a) Locality map of the Izu (I)–Bonin (B)–Mariana (M) Arc system. Location of the study area is shown by dashed rectangle. (b) Tectonic setting of the Mariana Arc–Trough system, Mariana Trough (CG = Central Graben, Spreading Ridge, SVTZ = Southern Volcano-Tectonic Zone, NVTZ = Northern Volcano-Tectonic Zone after Gribble *et al.* 1998), Mariana Arc (SSP = Southern Seamount Province, CIP = Central Island Province, NSP = Northern Seamount Province, after Stern *et al.* 1988), West Mariana Ridge (modified after Martinez and Taylor 2003; Stern *et al.* 2006). The Pacific Plate subducts beneath the Mariana Arc at the Mariana Trench (trench axis: broken line), where the 6000 m isobath is shown. Dredge locations in this study are shown as solid circles.

spreading-related back-arc basin basalts (BABB) from the southern Mariana Trough have mid-ocean ridge basalt (MORB)-like compositions (Gribble *et al.* 1996), while the genesis of basalts within the Central Graben is only studied in reconnaissance (Stern *et al.* 1996). It is well known that the majority of BABB are generated from regions of depleted mantle that is enriched in volatiles, Ba, Th, U, and Pb derived from the subducting slab (e.g. Stern *et al.* 1990; Saunders *et al.* 1991; Woodhead *et al.* 1993; Pearce *et al.* 1995; Gribble *et al.* 1998; Fretzdorff *et al.* 2002). Recently, Woodhead *et al.* (2012) indicated the importance of characterizing the "ambient mantle", prior to modification by slab-derived fluids or melts, in order to properly interpret the origins of subduction zone magmas. Mariana Arc magmas were generated as a result of partial melting of convecting asthenosphere above the subducting Pacific lithosphere and these arc lavas show that the mantle wedge was affected by the addition of subducted sediment melts or fluids released during dehydration of the oceanic crust or serpentinite (e.g. Stern *et al.* 1993; Elliott *et al.* 1997; Peate & Pearce 1998; Stern *et al.* 2006; Barnes *et al.* 2008; Kelley *et al.* 2010; Marske *et al.* 2011; Tamura *et al.* 2014).

In the present paper, we present new major and trace element, and Sr, Nd, and noble gas isotope data for fresh igneous rocks from the extensional axis of the Central Graben and Spreading Ridge in the Mariana Trough, from the magmatic front of the Mariana Arc, and from the southernmost Mariana forearc (Fig. 1). The new data contribute to our current understanding of the spatial geochemical variations between magma sources for arc and back-arc basins, from initial rifting through seafloor spreading. These spatial variations may be related to transport of slab-derived components into the mantle wedge over much wider areas above the subduction zone than is currently thought. We aim to identify the petrogenetic processes and the key components that control geochemical compositional variations in the mantle source of magmas in the Mariana Arc–Trough system. As mentioned before, a great deal of work has been done about radiogenic isotopic (e.g. Sr, Nd, and Pb) and trace elemental characteristics of samples from the Mariana Arc–Trough system, which identifies subduction-modified mantle and slab-derived components (e.g. Gribble *et al.* 1996; Elliott *et al.* 1997; Pearce *et al.* 2005; Stern *et al.* 2006; Tamura *et al.* 2014), whereas much less is known about noble gas

isotopic compositions (Sano *et al.* 1986, 1998; Ikeda *et al.* 1998). Noble gases have a pivotal role to play in addressing the volatile mass balance between the Earth's interior and exterior reservoirs (Hilton *et al.* 2002).

In this contribution, noble gas isotope data provide important information that enables the relative roles of mantle and subducted materials during magma generation to be understood, distinguishing between contributions from different recycled subducted reservoirs such as fluid and sediment melt components (Poreda 1985; Sano *et al.* 1986, 1998; Gasparon *et al.* 1994; Ikeda *et al.* 1998; Ikeda *et al.* 2001). The recycling efficiency of noble gases into the mantle is poorly known. Recent studies have revealed the recycling of heavy noble gases (Jambon *et al.* 1986; Ozima & Podosek 2002). This paper provides evidence for recycling of Kr and Xe through subduction zones and the arc. These data allow us to discuss the implications of the spatial variations from the magmatic front to the back-arc basin with respect to variations in mantle and slab-derived contributions.

GEOLOGIC SETTING AND SAMPLE LOCATIONS

The Mariana Arc–Trough system forms the southern half of the Izu–Bonin–Mariana (IBM) arc system, a 2500-km long intra-oceanic convergent margin extending from central Japan in the north to Guam in the south (Fig. 1). The IBM arc developed in response to subduction of the Pacific Plate beneath the Philippine Sea Plate. Dredge locations where samples were obtained for analysis during this study are shown in Figure 1 and listed in Table 1.

The Mariana Arc is subdivided into three provinces by Stern *et al.* (1988): the Northern Seamount Province (NSP, 20.7°N–24.0°N), the Central Islands Province (CIP, 16.0°N–20.7°N), and the Southern Seamount Province (SSP, south of 16.0°N). Igneous rock samples from the magmatic front were recovered on the Cook 07 expedition of the Scripps Institution of Oceanography research vessel (R/V) *Melville* during 2001, with dredged samples D50 and D41 from the CIP, and D65, D31, and D14 from the SSP. The compositions of some D50 basalts are also reported in Stern *et al.* (2006). Most samples are fresh basalts with plagioclase, clinopyroxene, and olivine phenocrysts, with a single cumulate-textured gabbro sample from D41 dominated by plagioclase, clinopyroxene, and olivine. Fresh cumulate-textured clinopyroxenite with minor interstitial olivine were sampled at D8 during the 2003 KH03-3 cruise of the University of Tokyo's R/V Hakuho Maru. This site lies on the landward slopes of the Mariana Trench and brings a sample of the southern Mariana forearc.

The Mariana Trough is an actively extending back-arc basin to the west of the Mariana Arc, with an extensional axis in the northern Mariana Trough that is propagating northwards into the NSP. Seafloor spreading characterizes extension in the south and rifting to the north of 19.7°N. Samples from the Spreading Ridge were obtained by dredging during the Cook 07 expedition, with sites D3 and D68 recovering pillow basalts with fresh glass. In addition, dredges D04, D06, D08, D11, D12, D19, D20, and D21 were collected from the extensional axis of the Central Graben during the 2002 KR02-01 expedition of the Japan Marine Science and Technology Center's R/V Kairei; this recovered pillow basalts with very fresh glass.

ANALYTICAL TECHNIQUES AND SAMPLE PREPARATION

Clean glass separates isolated from Mariana Trough pillow basalt rinds, bulk rock (free of Mn crust and alteration minerals) and olivine separates from the Mariana Arc basalt and gabbro were analyzed. The olivine formed phenocrysts in the basalt and gabbro. Clean olivine grains were handpicked from crushed rocks. Rock chips were rinsed in an ultrasonic bath and soaked in hydrogen peroxide with hot distilled de-ionized water for 1–3 weeks until the wash water remained clear following the addition of $AgNO_3$; this rinsing and soaking was undertaken to remove as much seawater contamination as possible. These rock chips, glassy pillow rinds from the Mariana Trough and bulk rocks from the Mariana Arc basalt and gabbro, and clinopyroxenite bulk rocks from the Mariana forearc were powdered in an agate mill for major and trace element, and Sr and Nd isotope analyses. Olivine grains (>1 mm) from the Mariana Arc basalt and gabbro, and clinopyroxenite (2–5 mm) bulk rocks from the Mariana forearc, and glassy pillow rinds (2–5 mm) from the Mariana Trough were cleaned ultrasonically in hydrogen peroxide, hot distilled de-ionized water, ethanol, and acetone prior to noble gas isotopic analysis.

The compositions of mineral phases in which noble gases were measured were analyzed using a

Table 1 Major element data of samples from the Mariana Arc and the Mariana Trough

Location	Mariana Arc								Forearc	Mariana Trough				
	Central Islands Province				Southern Seamount Province					Spreading Ridge				
	Mission				Cook Expedition 07				KH03-3	Cook Expedition 007				
Sample No.	D50-2-1	D41-1-1	D31-1-1	D31-2-3	D14-1-2	D14-1-4	D14-1-5	D65-2-2	D8-301	D3-4	D3-9	D68-2-1	D68-2-4	
Latitude N	17°24'10"	16°43'18"	15°35'12"		14°39'54"'			14°16'12"	11°48'24"	14°35'0"		14°10'12"		
Longitude E	145°42'5"	145°43'16"	145°34'51"'		145°0'0"			144°5'41"	143°26'26"	144°6'0"		143°58'6"		
Depth m	1,965-1,928	1,692-1,540	770-540		2,188-1,860			1,732-1,524	4,126-3,474	4,296-4,119		3,931-3,730		
Rock type	Basalt	Ol. Gabbro	Basalt	Basalt	Basalt	Basalt	Basalt	Basalt	Clinopyroxenite	Basalt Gl.	Basalt Gl.	Basalt Gl.	Basalt Gl.	
SiO_2	47.14	45.18	50.71	51.14	48.73	48.57	48.53	49.85	47.01	50.59	nd	49.66	nd	
TiO_2	0.68	0.16	0.82	0.70	0.48	0.47	0.48	0.76	0.21	1.74	nd	1.30	nd	
Al_2O_3	18.26	21.89	16.71	15.88	10.39	10.30	10.35	15.70	2.19	15.67	nd	15.71	nd	
Fe_2O_3	10.69	5.39	11.41	9.86	9.44	9.36	9.55	10.43	11.73	10.36	nd	9.66	nd	
MnO	0.17	0.09	0.20	0.18	0.16	0.16	0.16	0.16	0.22	0.17	nd	0.16	nd	
MgO	6.61	9.65	5.65	7.04	15.18	15.35	15.33	7.11	24.00	6.41	nd	7.79	nd	
CaO	13.94	16.94	10.95	12.27	14.31	14.44	14.16	12.42	14.27	10.45	nd	11.54	nd	
Na_2O	1.56	0.52	2.53	2.16	1.15	1.11	1.12	2.26	0.12	3.24	nd	3.16	nd	
K_2O	0.25	0.03	0.59	0.39	0.44	0.42	0.43	0.59	0.01	0.21	nd	0.11	nd	
P_2O_5	0.08	0.01	0.10	0.07	0.10	0.10	0.11	0.19	0.00	0.13	nd	0.12	nd	
Total	99.38	99.85	99.67	99.68	100.38	100.27	100.21	99.46	99.76	98.96		99.20		

Location	Mariana Trough														
	Central Graben														
	Mission									KR02-01					
Sample No.	D04-001	D06-002	D08-005	D08-006	D08-022	D08-303	D11-027	D12-031	D12-110	D12-116	D19-005	D20-107	D21-002	D21-003	D21-004
Latitude N	20°3'6"	20°3'22"	19°25'30"				20°17'20"	20°24'38"			21°6'36"	21°21'46"	21°36'32"		
Longitude E	143°57'12"	143°57'32"	144°28'44"				143°55'53"	143°56'48"			143°18'34"	143°16'59"	143°12'52"		
Depth m	4,606-4,451	4,459-4,438	4,638-4,454				4,228-4,160	4,132-4,089			4,300-4,239	4,047-3,751	3,384-3,252		
Rock type	Basalt Gl.	Basalt Gl.	Basalt Gl.	Basalt Gl.	Basalt Gl.	Basalt Gl.	Basalt Gl.	Basalt Gl.	Basalt Gl.	Basalt Gl.	Basalt Gl.	Basalt Gl.	Basalt Gl.	Basalt Gl.	Basalt Gl.
SiO_2	50.44	nd	50.52	50.54	50.64	50.51	49.28	50.70	49.82	49.76	51.10	50.44	50.83	50.79	50.66
TiO_2	1.16	nd	1.18	1.18	1.17	1.18	1.25	1.34	1.26	1.26	1.16	1.10	0.89	0.88	0.89
Al_2O_3	16.07	nd	15.82	15.88	15.78	15.71	16.10	16.33	16.79	16.91	15.92	15.56	16.05	16.02	15.87
Fe_2O_3	8.64	nd	8.55	8.54	8.55	8.64	8.79	8.73	8.72	8.74	8.62	8.62	8.36	8.36	8.38
MnO	0.15	nd	0.15	0.15	0.15	0.14	0.14	0.15	0.15	0.15	0.15	0.14	0.15	0.15	0.15
MgO	8.41	nd	9.11	8.94	9.16	8.95	9.05	7.81	8.91	9.00	9.16	8.54	9.98	9.96	10.04
CaO	11.07	nd	10.65	10.71	10.64	10.69	10.79	11.09	10.93	10.94	10.62	10.50	10.81	10.81	10.79
Na_2O	3.22	nd	2.94	2.96	2.95	2.62	2.90	3.33	3.32	3.30	3.06	2.57	2.56	2.58	2.55
K_2O	0.27	nd	0.34	0.35	0.33	0.32	0.17	0.35	0.21	0.21	0.43	0.31	0.67	0.66	0.66
P_2O_5	0.16	nd	0.17	0.16	0.16	0.12	0.11	0.19	0.16	0.16	0.19	0.11	0.19	0.19	0.19
Total	99.59		99.41	99.42	99.53	98.87	98.58	100.02	100.25	100.40	100.39	97.89	100.49	100.40	100.16

JEOL JCXA-733 electron microprobe at the Ocean Research Institute of the University of Tokyo, using a 15 kV accelerating voltage, 12 nA current, and 1 μm diameter beam size.

Major and trace element (Rb, Sr, Ba, Nb, Y, Zn, and Zr) concentrations of the whole rocks were determined by X-ray fluorescence (XRF) using a Rigaku RIX 3000 instrument at the National Institute of Polar Research, Tokyo, following analytical procedures outlined by Motoyoshi and Shiraishi (1995), Motoyoshi *et al.* (1996), and Seno *et al.* (2002). Other trace element concentrations in Mariana whole rocks were measured at Activation Laboratories Ltd. (Ontario, Canada) by inductively coupled plasma–mass spectrometry (ICP–MS).

Sr and Nd isotopic compositions of the whole rock samples were determined using a Finnigan MAT 262 solid source mass spectrometer at Niigata University, Japan, using the extraction procedures for Sr and Nd from rock powder suggested by Ikeda (2006). Sr isotopic compositions were fractionation-corrected to an $^{86}Sr/^{88}Sr$ value of 0.1194, and adjusted to a value of 0.710251 for the NBS987 (NIST SRM987) standard. $^{143}Nd/^{144}Nd$ ratios were normalized to an $^{146}Nd/^{144}Nd$ value of 0.7219 and are reported relative to the $^{143}Nd/^{144}Nd$ value (0.512115) for the Geological Survey of Japan JNdi-1 standard, corresponding to a $^{143}Nd/^{144}Nd$ value of 0.511858 for the LaJolla standard (Tanaka *et al.* 2000).

Samples for noble gas isotopic analysis (olivines from basalts and gabbros, and rock chips from the clinopyroxenite) weighing between 0.5 and 1.0 g were wrapped in 10 μm thick Al foil. Wrapped samples were placed inside a sample holder connected to an ultrahigh-vacuum line for noble gas extraction and purification. During extraction line baking, samples were heated to about 150 °C for more than a day to remove atmospheric contamination. Noble gases were extracted by melting the sample in a Mo crucible at 1800 °C, then purifying the extracted gases by exposure to hot Ti–Zr getters. The noble gases were then separated into two fractions (He + Ne and Ar + Kr + Xe) using a charcoal trap at liquid nitrogen temperatures, with Ne separated from He by adsorption onto a cryogenically cooled sintered stainless steel trap at 15 K. After He measurements, Ne was desorbed from the cryogenic trap at 45 K. The Ar + Kr + Xe fraction was desorbed from the charcoal and separated into each element using a cryogenic trap at 105 K (to trap Kr and Xe), 135 K (to trap Xe), and 230 K (to desorb Xe). Abundances and isotopic compositions were measured using a modified VG 5400 (MS-3) mass spectrometer at the University of Tokyo. Pipetted atmospheric noble gases and an HESJ $^{3}He/^{4}He$ gas standard (Matsuda *et al.* 2002) were used to determine sensitivities and mass discriminations for all noble gas isotopes. Typical blank levels during analysis were as follows: $^{4}He = 1 \times 10^{-10}$, $^{20}Ne = 4 \times 10^{-12}$, $^{40}Ar = 2 \times 10^{-9}$, $^{84}Kr = 2 \times 10^{-13}$, and $^{132}Xe = 8 \times 10^{-14}$ cm^3 STP (Standard Temperature and Pressure). Errors for isotope ratios were given at one standard deviation, and uncertainties for concentrations were estimated to be about ±10%.

RESULTS

MINERAL CHEMISTRY

The major element compositions of minerals that were analyzed for noble gases are presented in Appendix (Tables A1, A2). These include olivine phenocrysts from representative Mariana Arc samples (D14-1-2, D31-1-1, D31-2-3, D50-2-1, D65-2-2) as well as the olivine separates from the gabbro (D41-1-1) and clinopyroxenite (D8-301) and clinopyroxenes from the clinopyroxenite.

Olivines in sample D31-2-3 show a large range in forsterite content (Fo 77-90). Olivines in other samples including the gabbro and clinopyroxenite show limited variation in forsterite content (D50-2-1: Fo_{75}; D31-1-1: Fo_{74}; D14-1-2: $Fo_{87\text{-}90;}$ D65-2-2: Fo_{81}; D41-1-1 (gabbro): $Fo_{79\text{-}80;}$ D8-301 (clinopyroxenite): Fo_{79}). NiO contents in all olivines, including those from the gabbro and clinopyroxenite, are less than 0.17 wt% showing differentiation features. Clinopyroxenes in the clinopyroxenite (D8-301) are of almost constant composition (Mg = 83–84).

MAJOR AND TRACE ELEMENT VARIATIONS

The whole rock data are shown in Tables 1 and 2. Most Mariana Trough basalts define a low-K suite, whereas most Mariana Arc basalts define a medium-K suite (Fig. 2). The TiO_2 vs FeO*/MgO diagram (Fig. 3) shows that Mariana Trough basalts have higher Ti contents and fall in the field defined by MORB, whereas arc rocks contain less Ti. The Mariana Arc data with low FeO*/MgO (≈ 0.5) include the gabbro and clinopyroxenite, together with the picritic basalts (MgO ≈ 15 wt%; D14-1-2, D14-1-4, and D14-1-5).

Trace element variation diagrams show that patterns of N-MORB normalized trace elements become flatter from the Mariana Arc basalts and

Table 2 Trace element data of samples from the Mariana Arc and the Mariana Trough

Location	Mariana arc								Mariana Trough				
	Central Islands Province		Southern Seamount Province						Forearc		Spreading Ridge		
Sample No.	D50–2-1	D41–1-1	D31–1-1	D31–2-3	D14–1-2	D14–1-4	D14–1-5	D65–2-2	D8–301	D3–4	D3–9	D68–2-1	D68–2-4
V	344	125	334	288	264	300	302	298	156	278	338	232	218
Cr	100	80	90	190	1120	1390	1420	120	720	220	270	280	270
Co	36	52	49	34	66	76	77	42	86	39	47	41	38
Ni	40	140	70	50	270	330	330	60	220	110	140	120	100
Cu	120	30	200	130	70	90	100	150	10	70	80	80	80
Zn	80	50	120	120	90	100	100	130	70	140	150	120	100
Ga	17	17	24	16	13	14	15	17	3	22	26	19	16
Ge	1.5	1.5	2.1	1.6	2.2	2.3	2.2	1.6	1.8	1.5	1.7	1.7	1.2
Rb	4	1	11	6	7	6	7	12	ndt	3	3	1	ndt
Sr	293	329	346	287	359	398	408	313	97	208	234	176	263
Y	14.8	3.8	21.6	18.0	11.3	12.0	12.1	18.6	6.7	36.0	40.3	27.4	26.5
Zr	18	5	50	40	24	25	26	42	7	119	141	77	72
Nb	0.5	0.2	1.3	0.6	1.0	1.1	0.9	1.3	ndt	4.3	4.9	1.9	2.0
Ba	75	31	192	123	112	113	115	120	11	33	37	23	27
La	2.34	0.46	4.92	2.36	4.90	4.70	4.94	5.91	0.97	5.74	6.41	3.72	3.49
Ce	5.28	1.11	11.0	6.18	9.62	9.33	9.75	13.2	3.04	16.3	18.0	11.4	10.6
Pr	0.78	0.17	1.50	1.08	1.38	1.31	1.38	1.75	0.53	2.35	2.61	1.72	1.59
Nd	4.34	1.07	8.00	5.43	6.76	6.49	6.71	8.61	3.20	12.9	14.5	10.0	9.25
Sm	1.50	0.39	2.43	1.65	2.01	1.89	1.93	2.59	1.12	4.15	4.69	3.35	3.07
Eu	0.635	0.218	0.938	0.669	0.709	0.662	0.711	0.944	0.335	1.58	1.74	1.32	1.22
Gd	1.84	0.49	2.83	2.41	2.04	1.90	2.06	2.82	1.21	4.94	5.51	4.04	3.76
Tb	0.35	0.10	0.53	0.44	0.34	0.33	0.34	0.50	0.22	0.92	1.05	0.78	0.72
Dy	2.34	0.67	3.47	2.90	2.05	1.94	2.02	3.19	1.33	6.09	6.81	5.11	4.72
Ho	0.52	0.14	0.75	0.60	0.42	0.38	0.41	0.69	0.26	1.31	1.46	1.10	1.00
Er	1.59	0.40	2.26	1.78	1.21	1.14	1.21	2.08	0.78	3.91	4.33	3.25	3.00
Tm	0.237	0.055	0.328	0.265	0.173	0.164	0.175	0.307	0.110	0.571	0.637	0.471	0.441
Yb	1.45	0.34	2.09	1.72	1.08	1.04	1.09	1.96	0.67	3.55	4.00	2.96	2.74
Lu	0.222	0.051	0.317	0.266	0.160	0.153	0.157	0.300	0.101	0.531	0.595	0.428	0.403
Hf	0.7	0.2	1.4	1.3	0.8	0.8	0.7	1.4	0.4	3.2	3.6	2.4	2.2
Ta	0.01	ndt	0.05	ndt	0.04	0.05	0.04	0.05	ndt	0.25	0.27	0.10	0.10
Th	0.20	ndt	0.56	0.22	0.46	0.44	0.47	0.61	ndt	0.29	0.32	0.15	0.12
U	0.32	0.11	0.36	0.36	0.28	0.22	0.26	0.72	0.11	0.20	0.22	0.15	0.20

Table 2 *(Continued)*

Location	Mariana Trough																
	Central Graben																
Sample No.	D04–001	D06–002	D08–005	D08–006	D08–022	D08–303	D11–027	D12–031	D12–110	D12–116	D19–005	D20–107	D21–002	D21–003	D21–004	JA-1	JA-1 *
V	200	188	203	217	201	208	204	nd	205	192	265	267	238	218	219	136	105
Cr	260	230	320	330	310	310	320	nd	290	300	430	350	580	510	530	ndt	7.83
Co	32	28	33	35	31	32	36	nd	33	33	40	38	48	42	43	14	12.3
Ni	120	100	160	170	160	150	170	nd	150	160	190	170	270	250	240	ndt	3.49
Cu	70	60	60	70	90	70	80	nd	70	70	80	80	100	90	80	60	43
Zn	90	60	80	90		80	100	nd	80	90	100	110	110	90	90	120	90.9
Ga	15	13	15	16	15	15	17	nd	15	16	19	18	18	17	16	25	16.7
Ge	1.2	2.6	1.2	1.5	1.0	1.2	1.3	nd	1.6	1.4	1.4	1.6	1.7	1.5	1.4	1.7	1.33
Rb	5	8	5	6	5	5	3	nd	3	3	9	8	15	14	14	15	12.3
Sr	231	227	223	239	211	224	247	nd	240	242	331	313	332	299	293	311	263
Y	25.8	24.2	25.5	27.3	24.6	25.3	28.3	nd	27.8	27.6	29.8	27.8	20.2	19.4	19.0	30.4	30.6
Zr	109	105	106	112	105	105	125	nd	119	122	137	124	74	68	66	84	88.3
Nb	4.6	12.5	5.8	6.2	5.7	5.8	3.8	nd	3.6	3.6	5.5	4.8	4.1	4.1	3.8	1.7	1.85
Ba	53	51	53	58	53	53	46	nd	45	46	107	118	137	123	124	362	311
La	5.90	5.59	6.35	6.32	6.22	6.12	5.31	nd	5.22	5.42	8.74	7.34	10.3	10.3	9.88	5.54	5.24
Ce	15.3	14.7	15.4	15.4	15.1	15.2	14.6	nd	14.2	14.6	19.8	17.0	20.8	20.9	20.2	14.3	13.3
Pr	2.03	1.92	2.01	2.02	1.95	1.99	1.99	nd	1.97	1.99	2.43	2.11	2.49	2.50	2.40	2.03	1.71
Nd	10.4	10.1	10.3	10.2	9.98	10.2	10.8	nd	10.4	10.4	11.6	10.3	11.0	11.2	10.5	11.2	10.9
Sm	3.31	3.18	3.26	3.24	3.15	3.21	3.35	nd	3.35	3.40	3.35	3.13	3.07	3.14	2.98	3.54	3.52
Eu	1.29	1.20	1.25	1.25	1.21	1.21	1.30	nd	1.30	1.30	1.26	1.18	1.14	1.13	1.08	1.21	1.2
Gd	3.88	3.60	3.74	3.82	3.63	3.70	3.95	nd	3.90	3.92	3.71	3.48	3.17	3.20	3.06	3.98	4.36
Tb	0.70	0.67	0.70	0.69	0.67	0.67	0.74	nd	0.72	0.73	0.67	0.62	0.55	0.57	0.53	0.75	0.75
Dy	4.56	4.26	4.54	4.56	4.44	4.40	4.76	nd	4.65	4.73	4.23	4.01	3.59	3.61	3.37	4.97	4.55
Ho	0.96	0.89	0.98	0.98	0.92	0.96	1.01	nd	0.99	1.03	0.91	0.86	0.76	0.75	0.72	1.07	0.95
Er	2.87	2.71	2.91	2.93	2.77	2.85	3.03	nd	2.98	3.04	2.71	2.56	2.18	2.18	2.07	3.20	3.04
Tm	0.408	0.398	0.411	0.408	0.407	0.412	0.435	nd	0.432	0.451	0.395	0.378	0.315	0.310	0.302	0.473	0.47
Yb	2.65	2.46	2.63	2.70	2.56	2.58	2.76	nd	2.76	2.79	2.45	2.37	1.98	1.98	1.90	3.05	3.03
Lu	0.390	0.361	0.387	0.401	0.375	0.388	0.412	nd	0.408	0.411	0.375	0.353	0.297	0.300	0.287	0.460	0.47
Hf	2.3	2.3	2.3	2.4	2.3	2.3	2.5	nd	2.4	2.5	2.3	2.2	1.9	1.9	1.8	2.5	2.42
Ta	0.24	1.09	0.30	0.31	0.29	0.31	0.17	nd	0.17	0.17	0.21	0.18	0.22	0.27	0.21	0.08	0.13
Th	0.45	0.48	0.45	0.46	0.47	0.46	0.34	nd	0.33	0.33	0.78	0.74	1.10	1.11	1.04	0.78	0.82
U	0.23	0.39	0.23	0.24	0.24	0.23	0.19	nd	0.18	0.18	0.30	0.28	0.44	0.48	0.42	0.47	0.34

JA-1, Standard sample of Geological Survey of Japan; JA-1*, recommended values of JA-1 by Geological Survey of Japan (Imai *et al.* 1995); ndt, not detected; nd, not determined.

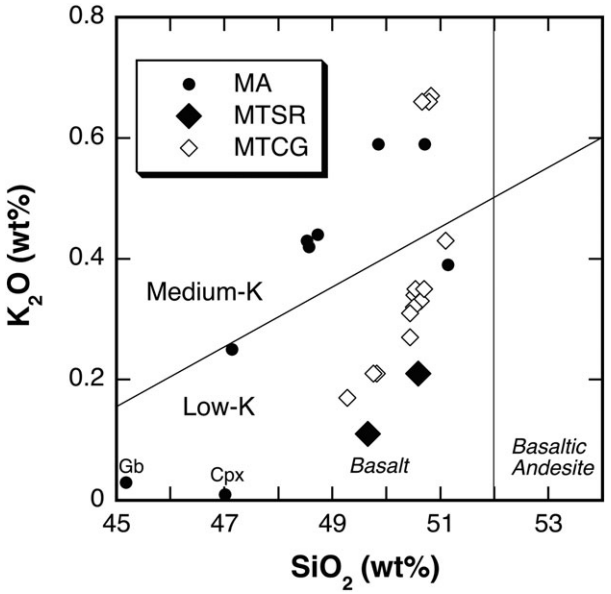

Fig. 2 K_2O vs SiO_2 diagram for samples from the Mariana Arc and the Mariana Trough. The silica and K_2O boundaries are from LeMaitre (1989). MA, basalts from the Mariana Arc including gabbro (Gb) from the Central Islands Province and clinopyroxenite (Cpx) from the forearc; MTSR, basalts from the Mariana Trough Spreading Ridge; MTCG, basalts from the Mariana Trough Central Graben.

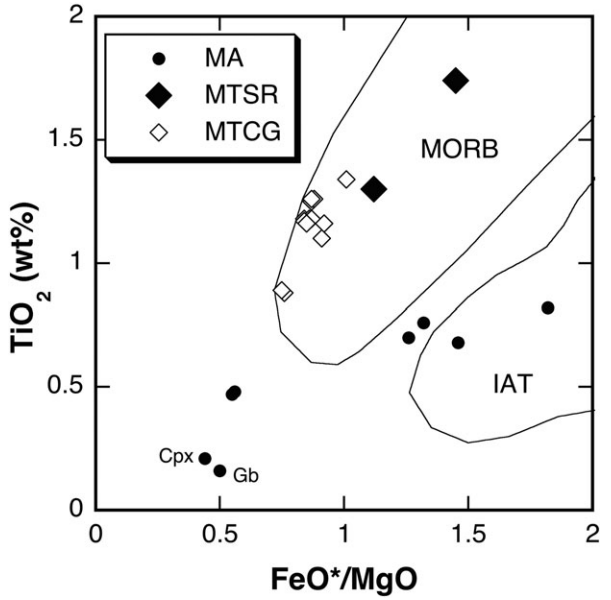

Fig. 3 TiO_2 vs FeO*/MgO diagram for samples from the Mariana Arc and the Mariana Trough. Field boundaries for MORB and Island Arc Tholeiite (IAT) are from Ikeda and Yuasa (1989). Symbols are the same as those in Fig. 2.

igneous rocks (MA, including the gabbro and clinopyroxenite) through basalts of the Mariana Trough Central Graben (MTCG) to basalts of the Mariana Trough Spreading Ridge (MTSR) (Fig. 4 shows mean values). They all have an identifiable arc signature, exhibiting enrichments in fluid

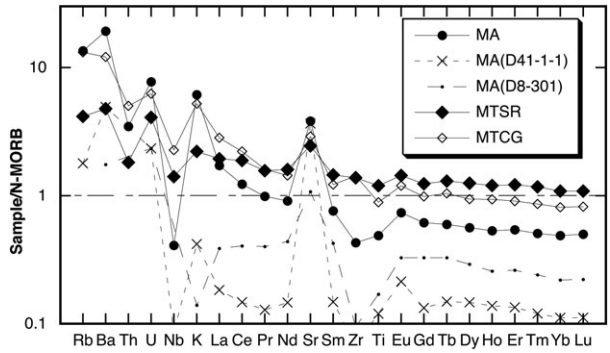

Fig. 4 Trace element variation diagram, arranged in order of increasingly incompatible elements to the left. N-MORB normalizing values after Sun and McDonough (1989). Symbols are the same as those in Fig. 2. Basalts from MA, MTSR, and MTCG are shown as mean values. Mariana Arc samples D41-1-1 (olivine gabbro from the Central Islands Province) and D8-301 (clinopyroxenite from the forearc) are cumulate rocks.

mobile elements (Rb, Ba, U, K, and Sr) and depletions in high field strength incompatible elements (Nb, Zr, and heavy REE) as described by Stern *et al.* (2003).

Sr AND Nd ISOTOPE VARIATIONS

The Sr and Nd isotope analyses are shown in Table 3 and Figure 5. Mariana Trough basalts (MTSR and MTCG) show MORB-like compositions that plot on an upper mantle Sr–Nd correlation line (SNUM; Gill 1981). This can reflect mixing between oceanic sediments and depleted MORB-type mantle (e.g. Stern *et al.* 2006). In comparison, Mariana Arc samples (including the gabbro and clinopyroxenite) are displaced towards higher $^{87}Sr/^{86}Sr$ values for given $^{143}Nd/^{144}Nd$ values along a trend characteristic of influence from subducted seawater, which is generally observed within arc rocks (e.g. DePaolo 1988; Stern *et al.* 1993).

NOBLE GAS ISOTOPE VARIATIONS

Noble gas isotope analyses are shown in Tables 4 and 5. With the exception of a few samples, $^3He/^4He$ ratios (MORB-like compositions) are remarkably uniform regardless of ^4He concentrations (average 1.2×10^{-5}; Kurz 1991; Fig. 6) that is maintained across a 9000-fold range. This trend cannot result from degassing and subsequent ingrowth of radiogenic ^4He during magmatic differentiation, from post-eruptive contamination with seawater-derived atmospheric helium, or from diffusive loss of magmatic helium. It most likely reflects the He isotopic signatures of magma

Table 3 Sr and Nd isotopic data of samples from the Mariana Arc and the Mariana Trough

Sample No.	$^{87}Sr/^{86}Sr$ 2σ	$^{143}Nd/^{144}Nd$ 2σ
Mariana arc (Central Islands Province)		
D50–2-1	0.703776 ± 13	0.513004 ± 14
D41–1-1	0.703555 ± 13	0.512946 ± 13
Mariana arc (Southern Seamount Province)		
D31–1-1	0.703614 ± 13	0.512997 ± 14
D31–2-3	0.703797 ± 10	0.513072 ± 14
D14–1-2	0.703537 ± 14	0.512954 ± 14
D14–1-4	0.703561 ± 9	0.512949 ± 17
D14–1-5	0.703510 ± 14	0.512948 ± 14
D65–2-2	0.704196 ± 13	0.512995 ± 14
Mariana arc (Forearc)		
D8–301	0.704421 ± 17	0.512894 ± 14
Southern Mariana Trough (Spreading Ridge)		
D3–4	0.702981 ± 14	0.513125 ± 14
D3–9	0.702954 ± 13	0.513136 ± 14
D68–2-1	0.702998 ± 14	0.513116 ± 13
D68–2-4	0.702955 ± 14	0.513114 ± 13
Northern Mariana Trough (Central Graben)		
D4–001	0.702989 ± 13	0.513112 ± 14
D6–002	0.703052 ± 13	0.513091 ± 13
D8–005	0.703022 ± 11	0.513073 ± 14
D8–006	0.702985 ± 12	0.513087 ± 14
D8–022	0.703064 ± 10	0.513077 ± 14
D8–303	0.703077 ± 14	0.513085 ± 14
D11–027	0.702993 ± 11	0.513118 ± 14
D12–031	0.703011 ± 11	0.513124 ± 14
D12–110	0.702989 ± 9	0.513091 ± 14
D12–116	0.702985 ± 14	0.513113 ± 24
D19–005	0.703175 ± 13	0.513029 ± 14
D20–107	0.703178 ± 14	0.513036 ± 14
D21–002	0.703427 ± 13	0.512873 ± 14
D21–003	0.703464 ± 12	0.512962 ± 14
D21–004	0.703464 ± 14	0.512953 ± 14

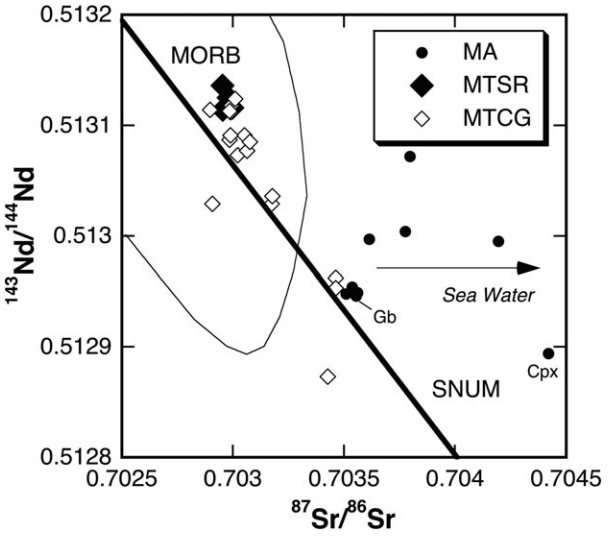

Fig. 5 $^{143}Nd/^{144}Nd$ vs $^{87}Sr/^{86}Sr$ diagram for samples from the Mariana Arc and the Mariana Trough. MORB field is compiled from DePaolo (1988) and Elliott *et al.* (1997). Symbols are the same as those in Fig. 2.

sources, as discussed for Lau Basin basalts by Honda *et al.* (1993a). In contrast, the few Mariana Arc samples with low $^{3}He/^{4}He$ ratios and ^{4}He concentrations less than 2×10^{-9} cc/g do not have average MORB isotopic compositions; these lower $^{3}He/^{4}He$ ratios can be due to radiogenic ingrowth of ^{4}He after magma formation. Atmospheric contamination including seawater does not significantly affect the $^{3}He/^{4}He$ ratios because $^{4}He/^{20}Ne$ ratios of these samples are greater than 12 (Table 4) as discussed by Sano and Wakita (1985).

Neon isotopic compositions are illustrated on a three-isotope plot ($^{20}Ne/^{22}Ne$ versus $^{21}Ne/^{22}Ne$) in Figure 7, and indicate that Mariana Arc samples contain atmospheric neon, whereas most Mariana Trough samples plot on the MORB array trend (Sarda *et al.* 1988) and the Manus Basin trend (Shaw *et al.* 2001) as shown in Ikeda *et al.* (1998) and Sano *et al.* (1998). One Central Graben sample (D08-303), which has extreme enrichments in $^{20}Ne/^{22}Ne$ and $^{21}Ne/^{22}Ne$, lies along the Lau Basin trajectory (Honda *et al.* 1993b), suggesting incorporation of solar-type Ne in the magma source as shown by Sano *et al.* (1998). This indicates binary mixing between two end-members (atmospheric and mantle neon), with the latter being a mixture of solar and nucleogenic neon in various proportions (Honda *et al.* 1993b; Hilton *et al.* 2002).

The $^{40}Ar/^{36}Ar$ ratios of Mariana Arc samples vary from atmospheric values to as high as 959, whereas Mariana Trough samples have a wider range of ratios, from atmospheric values to 3024. The Mariana Trough samples we analyzed have ratios similar to published Mariana Trough analyses (360–3869: Sano *et al.* 1986; Ikeda *et al.* 1998), as well as BABB from the Lau Basin (300–2430: Honda *et al.* 1993b), but are much lower than the maximum MORB $^{40}Ar/^{36}Ar = 28\,000$ (Staudacher *et al.* 1989). The $^{3}He/^{4}He$ and $^{40}Ar/^{36}Ar$ ratios can be explained by simple mixing between MORB and atmospheric components (Fig. 8). $^{40}Ar^*$ (radiogenic argon) concentrations are plotted against $^{4}He/^{40}Ar^*$ ratios in Figure 9. It is assumed that unfractionated magmas derived from mantle sources should have constant $^{4}He/^{40}Ar^*$ ratios, as this ratio is controlled by the K/U and Th/U ratios of the mantle (Allègre *et al.* 1986; Hanyu *et al.* 2005), with a predicted $^{4}He/^{40}Ar^*$ production ratio of between 2 and 5 (Ozima & Podosek 2002; Hanyu *et al.* 2005). The $^{4}He/^{40}Ar^*$ ratios of most Mariana Arc samples (0.04–4.9) are compatible with this production ratio value, whereas the $^{4}He/^{40}Ar^*$ ratios of Mariana Trough glass samples are much higher (2.6–206). These high values for the Mariana Trough samples were previously ex-

Table 4 Noble gas concentrations (He, Ne, Ar, Kr, and Xe) and isotopic ratios (He, Ne, and Ar) data of samples from the Mariana Arc and the Mariana Trough

Sample	Material	Mass (g)	^{3}He (10^{-15} ccSTP/g)	^{4}He (10^{-9} ccSTP/g)	^{3}He/^{4}He (x10^{-6})	R/R_A	^{20}Ne (10^{-9} ccSTP/g)	^{20}Ne/^{22}Ne	^{21}Ne/^{22}Ne	^{4}He/^{20}Ne	^{36}Ar (10^{-9} ccSTP/g)	^{40}Ar (10^{-9} ccSTP/g)	^{38}Ar/^{36}Ar	^{40}Ar/^{36}Ar	^{84}Kr (10^{-12} ccSTP/g)	^{132}Xe (10^{-12} ccSTP/g)
Mariana arc (Central Islands Province)																
D50–2-1	Olivine	0.8261	36.5	3.15	11.6 ± 1.4	8.3	0.016	nd	nd	197	0.162	48.8	0.18952 ± 0.00068	301.90 ± 0.25	4.14	0.48
D41–1-1	Olivine	0.8317	39.4	3.94	10.0 ± 1.4	7.1	0.142	9.83 ± 0.11	0.0294 ± 0.0021	28	0.180	54.5	0.18926 ± 0.00069	303.57 ± 0.62	4.64	0.158
Mariana arc (Southern Seamount Province)																
D31–1-1	Olivine	0.6483	3.3	0.65	5.04 ± 1.46	3.6	0.054	9.82 ± 0.18	0.0285 ± 0.0031	12	0.224	66.9	0.18899 ± 0.00085	298.55 ±0.34	3.60	0.19
D31–2-3	Olivine	0.5128	13.6	1.64	8.29 ± 1.48	5.9	0.050	nd	nd	33	0.533	159.0	0.18910 ± 0.00043	298.12 ± 0.34	115	9.59
D14–1-2	Olivine	1.0210	121	10.8	11.19 ± 0.92	8.0	0.021	nd	nd	514	0.106	33.9	0.18951 ± 0.00048	320.66 ± 0.47	7.75	
D14–1-4	Olivine	0.8803	203	16.9	12.00 ± 0.60	8.6	0.108	9.79 ± 0.07	0.0294 ± 0.0022	156	0.237	73.6	0.18906 ± 0.00043	311.05 ± 0.60	6.03	0.20
D14–1-5	Olivine	0.9331	240	19.9	12.07 ± 0.81	8.6	0.064	9.80 ± 0.25	0.02894 ±0.00182	313	0.170	55.4	0.18941 ± 0.00081	326.24 ± 0.73	4.59	0.151
D65–2-2	Olivine	0.9877	38.5	4.00	9.6 ± 1.16	6.9	0.091	9.84 ± 0.16	0.0292 ± 0.0025	44	0.168	50.6	0.18888 ± 0.00092	300.35 ± 0.64	4.26	0.19
D8–301	clinopyroxenite	1.1545	455	46.2	9.85 ± 0.39	7.0	0.184	9.93 ± 0.12	0.0307 ± 0.0012	251	1.657	1590.0	0.18969 ± 0.00073	959.63 ± 2.80	72.7	5.14
Mariana Trough (Spreading Ridge)																
D3–4	Glass	0.3353	118653	9303	12.75 ± 0.10	9.1	0.586	10.18 ± 0.07	0.0309 ± 0.0015	15875	1.366	801.9	0.18714 ± 0.00280	586.87 ± 3.68	23.77	1.09
D3–9	Glass	0.2906	115421	8870	13.01 ± 0.10	9.3	0.267	10.19 ± 0.10	0.0366 ± 0.0015	33233	0.288	475.4	0.19016 ± 0.00084	1649.7 ± 27.8	6.95	0.38
D68–2-1	Glass	0.4586	47034	3900	12.06 ± 0.08	8.6	2.000	9.69 ± 0.04	0.0299 ± 0.0007	1950	19.073	7120.0	0.18869 ± 0.00042	373.30 ± 0.43	69.1	2.37
D68–2-4	Glass	0.1092	48911	3847	12.71 ± 0.10	9.1	0.111	11.57 ± 0.69	0.0493 ± 0.0068	34805	0.132	195.8	0.18870 ± 0.00084	1488.5 ± 141.0	2.84	nd
Mariana Trough (Central Graben)																
D04–001	Glass	0.3220	100770	8306	12.13 ± 0.10	8.7	0.232	9.86 ± 0.10	0.0337 ± 0.0016	35877	0.243	145.4	0.18774 ± 0.00058	597.97 ± 6.61	5.65	0.37

Table 4 *(Continued)*

Sample	Material	Mass (g)	^{3}He (10^{-15} ccSTP/g)	^{4}He (10^{-9} ccSTP/g)	^{3}He/^{4}He (x10^{-6})	R/ R_A	^{20}Ne (10^{-9} ccSTP/g)	^{20}Ne/ ^{22}Ne	^{21}Ne/ ^{22}Ne	^{4}He/ ^{20}Ne	^{36}Ar (10^{-9} ccSTP/g)	^{40}Ar (10^{-9} ccSTP/g)	^{38}Ar/ ^{36}Ar	^{40}Ar/ ^{36}Ar	^{84}Kr (10^{-12} ccSTP/g)	^{132}Xe (10^{-12} ccSTP/g)
D06–002	Glass	0.4648	51048	4063	12.56 ± 0.10	9.0	0.073	10.73 ± 0.20	0.0403 ± 0.0029	55711	0.084	78.6	0.18852 ± 0.00095	934.05 ± 27.7	1.72	0.17
D08–005	Glass	0.4660	346657	28101	12.34 ± 0.11	8.8	2.197	9.83 ± 0.02	0.0297 ± 0.0004	12791	4.194	1429.4	0.19153 ± 0.00227	340.85 ± 0.28	96.11	4.77
D08–006	Glass	0.4960	328925	25599	12.85 ± 0.11	9.2	1.246	10.11 ± 0.03	0.0330 ± 0.0023	20545	0.864	461.7	0.18773 ± 0.00060	534.53 ± 2.78	nd	nd
D08–022	Glass	0.7132	320325	24764	12.93 ± 0.10	9.2	0.588	10.05 ± 0.03	0.0325 ± 0.0011	42122	0.889	468.0	0.18826 ± 0.00037	526.52 ± 0.76	20.96	1.10
D08–303	Glass	0.4149	350382	27657	12.67 ± 0.10	9.1	0.080	12.55 ± 0.36	0.0453 ± 0.0030	346169	0.116	257.1	0.19040 ± 0.00184	2207.7 ± 68.2	3.50	0.19
D11–027	Glass	0.2699	300776	23813	12.63 ± 0.10	9.0	0.619	10.11 ± 0.12	0.0334 ± 0.0018	38454	0.786	634.8	0.18969 ± 0.00052	808.06 ± 9.44	18.84	1.07
D12–031	Glass	0.4292	145800	11472	12.71 ± 0.10	9.1	0.130	10.87 ± 0.16	0.0442 ± 0.0028	88354	0.038	122.3	0.19182 ± 0.00171	3200.1 ± 301.0	4.10	0.25
D12–110	Glass	0.4288	186545	15162	12.30 ± 0.11	8.8	0.197	10.31 ± 0.12	0.0399 ± 0.0007	77091	0.190	575.9	0.19327 ± 0.00112	3024.4 ± 57.6	6.02	0.23
D12–116	Glass	0.6924	191058	15166	12.60 ± 0.11	9.0	0.338	9.91 ± 0.05	0.0343 ± 0.0009	44850	0.485	575.2	0.18865 ± 0.00073	1184.9 ± 5.1	36.71	8.11
D19–005	Glass	0.4745	13536	1150	11.77 ± 0.10	8.4	0.115	nd	nd	10000	0.353	110.0	0.18990 ± 0.00074	311.25 ± 0.50	9.58	1.04
D20–107	Glass	0.5085	3294	270	12.20 ± 0.26	8.7	0.333	9.73 ± 0.10	0.0302 ± 0.0016	811	0.615	183.0	0.18799 ± 0.00042	297.74 ± 0.65	15.2	0.49
D21–002	Glass	1.4401	1705	141	12.09 ± 0.09	8.6	0.051	9.73 ± 0.08	0.0299 ± 0.0021	2765	0.583	176.0	0.18956 ± 0.00047	301.97 ± 0.31	41.1	4.08
D21–003	Glass	0.5896	1203	101	11.91 ± 0.24	8.5	0.113	nd	nd	894	0.230	69.4	0.18900 ± 0.00058	301.29 ± 0.71	6.80	0.24
D21–004	Glass	0.9829	1290	108	11.94 ± 0.31	8.5	0.006	nd	nd	18000		nd			nd	nd

nd, not determined; R/RA, The measured ^{3}He/^{4}He ratio (R) is normalized to atmospheric helium isotope ratio R_A (1.4×10^{-6}).

Table 5 Isotopic compositions of Kr and Xe data of samples from the Mariana Arc and the Mariana Trough

Sample	$^{78}Kr/^{84}Kr$	$^{80}Kr/^{84}Kr$	$^{82}Kr/^{84}Kr$	$^{83}Kr/^{84}Kr$	$^{86}Kr/^{84}Kr$	$^{124}Xe/^{132}Xe$	$^{126}Xe/^{132}Xe$	$^{128}Xe/^{132}Xe$	$^{129}Xe/^{132}Xe$	$^{130}Xe/^{132}Xe$	$^{131}Xe/^{132}Xe$	$^{134}Xe/^{132}Xe$	$^{136}Xe/^{132}Xe$
Mariana arc (Southern Seamount Province)													
D31–2-3	0.00663	0.04053	0.2022	0.1986	0.29740	0.0044	0.0033	0.0738	0.994	0.1561	0.8161	0.3938	0.3260
	± 0.00233	± 0.00092	± 0.0023	± 0.0035	± 0.00418	± 0.0006	± 0.0007	± 0.0039	± 0.016	± 0.0031	± 0.0162	± 0.0106	± 0.0096
D14–1-5	nd	0.03939	0.2055	0.2030	0.29252	nd	nd	nd	nd	nd	nd	nd	nd
		± 0.00116	± 0.0034	± 0.0069	± 0.01010								
Mariana Trough (Spreading Ridge)													
D3–4	0.00630	0.03888	0.2014	0.1973	0.29942	0.0039	0.0034	0.0696	0.980	0.1482	0.7932	0.3798	0.3213
	± 0.00026	± 0.00055	± 0.0023	± 0.0022	± 0.00362	± 0.0007	± 0.0006	± 0.0031	± 0.017	± 0.0075	± 0.0209	± 0.0108	± 0.0047
D3–9	0.00628	0.04024	0.2022	0.1979	0.30048	0.0072	0.0039	0.0712	0.947	0.1480	0.7525	0.3775	0.3219
	± 0.00026	± 0.00102	± 0.0029	± 0.0040	± 0.00268	± 0.0025	± 0.0014	± 0.0044	± 0.040	± 0.0131	± 0.0356	± 0.0124	± 0.0245
D68–2-4	nd	0.03908	0.2143	0.2046	0.28981	nd	nd	nd	nd	nd	nd	nd	nd
		± 0.00359	± 0.0112	± 0.0131	± 0.01018								
Mariana Trough (Central Graben)													
D04–001	0.00671	0.04046	0.2065	0.1986	0.29990	0.0052	0.0044	0.0760	1.011	0.1549	0.8043	0.3759	0.3084
	± 0.00030	± 0.00094	± 0.0031	± 0.0040	± 0.00270	± 0.0010	± 0.0013	± 0.0082	± 0.053	± 0.0122	± 0.0683	± 0.0342	± 0.0148
D06–002	0.00714	0.03969	0.2035	0.1966	0.28838	0.0073	0.0037	0.0704	0.939	0.1531	0.7886	0.3902	0.3280
	± 0.00070	± 0.00226	± 0.0051	± 0.0037	± 0.01057	± 0.0031	± 0.0023	± 0.0055	± 0.038	± 0.0296	± 0.0421	± 0.0305	± 0.0135
D08–005	0.00611	0.03902	0.2008	0.1963	0.29651	0.0037	0.0035	0.0714	0.986	0.1511	0.7959	0.3901	0.3284
	± 0.00008	± 0.00026	± 0.0009	± 0.0007	± 0.00162	± 0.0003	± 0.0005	± 0.0013	± 0.006	± 0.0016	± 0.0093	± 0.0042	± 0.0027
D08–022	0.00620	0.03913	0.2003	0.1984	0.29796	0.0036	0.0035	0.0699	0.986	0.1502	0.7894	0.3850	0.3213
	± 0.00017	± 0.00030	± 0.0011	± 0.0007	± 0.00192	± 0.0005	± 0.0003	± 0.0024	± 0.023	± 0.0041	± 0.0136	± 0.0049	± 0.0051
D08–303	0.00649	0.04023	0.2022	0.2013	0.29511	0.0075	0.0035	0.0774	1.014	0.1476	0.7728	0.3841	0.3140
	± 0.00042	± 0.00105	± 0.0038	± 0.0036	± 0.00551	± 0.0022	± 0.0017	± 0.0117	± 0.055	± 0.0144	± 0.0639	± 0.0407	± 0.0327
D11–027	0.00623	0.39653	0.1977	0.1964	0.29812	0.0044	0.0033	0.0692	0.981	0.1558	0.8049	0.3898	0.3330
	± 0.00024	± 0.00382	± 0.0011	± 0.0015	± 0.00196	± 0.0008	± 0.0006	± 0.0030	± 0.032	± 0.0099	± 0.0158	± 0.0182	± 0.1195
D12–031	0.00639	0.04018	0.1996	0.2004	0.29584	0.0062	0.0042	0.0704	1.035	0.1530	0.8354	0.4104	0.3323
	± 0.00130	± 0.00174	± 0.0020	± 0.0037	± 0.00443	± 0.0021	± 0.0009	± 0.0068	± 0.057	± 0.0155	± 0.0468	± 0.0216	± 0.0299
D12–110	0.00696	0.04089	0.2000	0.1998	0.29811	0.0072	0.0030	0.0667	0.964	0.1520	0.7384	0.3725	0.3101
	± 0.00046	± 0.00100	± 0.0023	± 0.0037	± 0.00684	± 0.0035	± 0.0016	± 0.0098	± 0.048	± 0.0138	± 0.0817	± 0.0193	± 0.0184
D12–116	0.0062	0.03895	0.1994	0.1975	0.29630	0.0034	0.0034	0.0705	0.983	0.1509	0.7866	0.3907	0.3245
	± 0.0001	± 0.00029	± 0.0010	± 0.0010	± 0.00112	± 0.0001	± 0.0002	± 0.0007	± 0.006	± 0.0019	± 0.0055	± 0.0015	± 0.0019
Atmosphere	0.00609	0.03960	0.2022	0.2014	0.3052	0.00354	0.0033	0.07136	0.9832	0.15136	0.7890	0.3879	0.3294

nd, not determined.

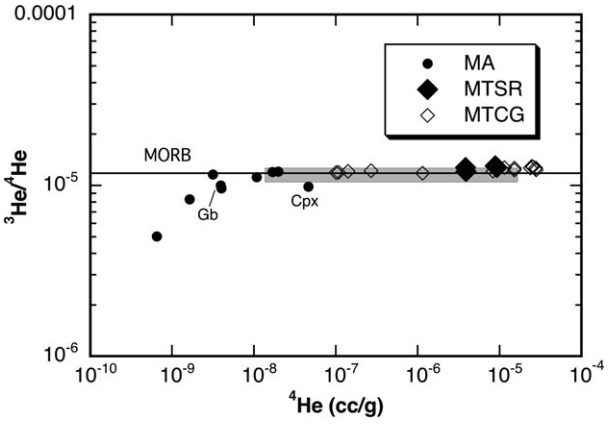

Fig. 6 ^{3}He/^{4}He vs ^{4}He concentrations for samples from the Mariana Arc and the Mariana Trough. Average MORB ^{3}He/^{4}He ratio from Kurz (1991). The shaded zone is the compositional range of Mariana Trough basalt from Ikeda *et al.* (1998). Symbols are the same as those in Fig. 2.

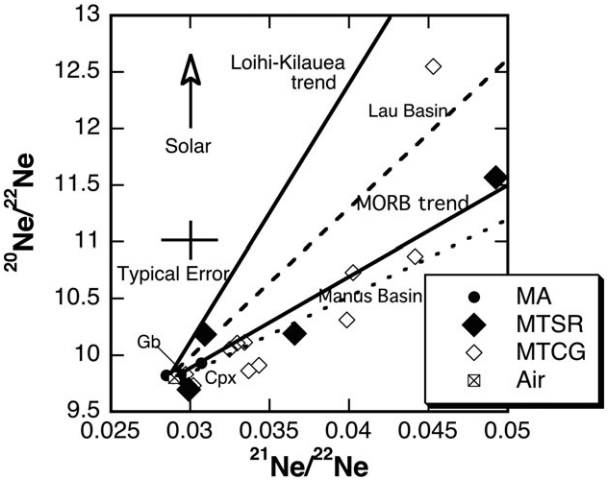

Fig. 7 ^{20}Ne/^{22}Ne vs ^{21}Ne/^{22}Ne diagram for samples from the Mariana Arc and the Mariana Trough. MORB and Loihi–Kilauea correlation lines are as given by Sarda *et al.* (1988). Data of Lau Basin trend and Manus Basin trend are from Honda *et al.* (1993) and Shaw *et al.* (2001), respectively. Symbols are the same as those in Fig. 2.

plained by elemental fractionation within the magma by vesiculation after partial melting of the mantle (Jambon *et al.* 1986; Sarda & Graham 1990). In addition, high ^{4}He/^{40}Ar* ratios coupled with lower ^{40}Ar* values for the Mariana Arc and Trough samples can be explained by solubility-controlled degassing, as is often observed in MORB (Jambon *et al.* 1986; Moreira & Sarda 2000; Burnard *et al.* 2002).

Mariana Arc and Mariana Trough samples have krypton and xenon isotope ratios that are similar to atmospheric values, indicating minimal mass fractionation effects, although correlated excesses in ^{129}Xe are found in some Central Graben samples (D04-001, D08-303, D12-031), similar to those found in BABB and MORB by Ikeda *et al.* (1998)

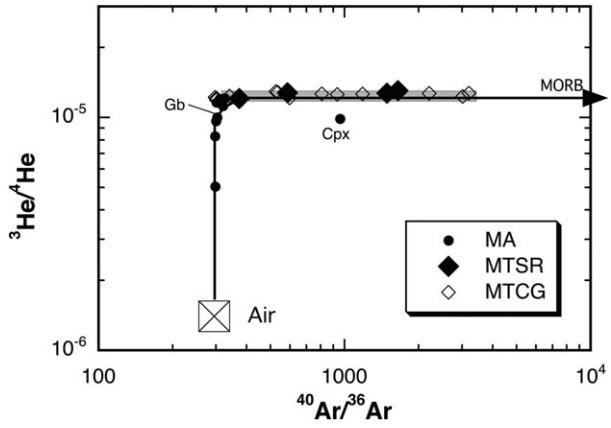

Fig. 8 ^{3}He/^{4}He vs ^{40}Ar/^{36}Ar diagram for samples from the Mariana Arc and the Mariana Trough. The curved line represents two-component mixing between MORB source and atmosphere (Air) (Kaneoka & Takaoka 1985). The shaded zone is the compositional range of Mariana Trough basalt from Ikeda *et al.* (1998) and Sano *et al.* (1998). Symbols are the same as those in Fig. 2.

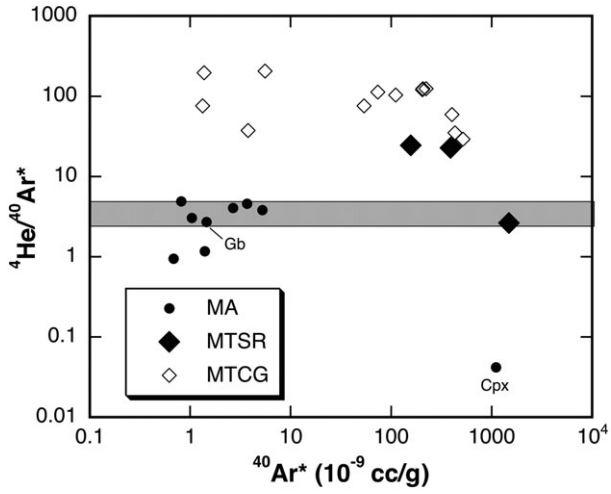

Fig. 9 ^{4}He/^{40}Ar* vs ^{40}Ar* diagram for samples from the Mariana Arc and the Mariana Trough. The shaded zone is the production ratio (Ozima & Podosek 2002; Hanyu *et al.* 2005). Symbols are the same as those in Fig. 2.

and Staudacher and Allègre (1982). One sample (D08-303) also shows excesses of ^{20}Ne and ^{21}Ne, suggesting primordial noble gases in the mantle source.

DISCUSSION

IMPLICATIONS FOR MANTLE COMPONENTS IN THE MARIANA ARC–TROUGH SYSTEM

The mantle wedge beneath the Mariana Arc and the Mariana Trough has geochemical and isotopic compositions indicating that it is relatively depleted in high field strength elements such as Nb,

relative to MORB, as is generally observed in convergent margin melts.

Incompatible elements such as Rb, K, Ba, Pb, and U are preferentially partitioned into aqueous fluids derived from the subducted slab. In contrast, high field strength incompatible elements such as Nb, Zr, and heavy rare earth elements are depleted in convergent margin magmas. Nb is probably mobilized from a rutile-bearing slab only by melting (Pearce *et al.* 2005). Thus, incompatible element ratios such as Ba/Th, La/Sm, U/Th, and Zr/Nb can discriminate between the two components responsible for most of the compositional variations observed in subduction zone magmas (e.g. Fretzdorff *et al.* 2002; Elliott 2003; Pearce *et al.* 2005; Stern *et al.* 2006); i.e. fluid-dominated (high Ba/Th and U/Th) and sediment melt dominated (high La/Sm and low Zr/Nb) components (Figs 10, 11). Mariana Arc basalts have compositions indicating both fluid and sediment melt contribute to a depleted mantle source, as discussed in recent investigations of Mariana Arc lavas (Hole *et al.* 1984; Elliott *et al.* 1997; Peate & Pearce 1998; Tollstrup & Gill 2005; Wade *et al.* 2005; Stern *et al.* 2006; Tamura *et al.* 2014), with the fluid component dominating in most Mariana Arc samples. This fluid component is thought to be derived from subducted sediments, altered oceanic crust, and the dehydration of subducted serpentinite (e.g. Elliott *et al.* 1997; Peate & Pearce 1998; Stern *et al.* 2006; Barnes *et al.* 2008). Mariana Trough Spreading Ridge basalts have MORB-like features and plot along a mixing trajectory between MORB sources and slab-derived fluids, potentially derived from altered oceanic crustal material. This is consistent with a model including a volatile-rich component in the generation of Mariana Trough basaltic magmas (Hawkins & Melchior 1985; Sano *et al.* 1986; Volpe *et al.* 1987; Hawkins *et al.* 1990; Stolper & Newman 1994; Gribble *et al.* 1996; Ikeda *et al.* 1998; Sano *et al.* 1998; Macpherson *et al.* 2000; Pearce *et al.* 2005). Basalts from the Mariana Trough Central Graben are also MORB-like but again trend away from MORB compositions toward both fluid and sediment melt compositions. The magmatic expression of the earliest Mariana Trough rifting (23°N–21°N: Northern Volcano-Tectonic Zone and Southern Volcano-Tectonic Zone) is largely indistinguishable from Mariana Arc lavas (Stern *et al.* 1990; Gribble *et al.* 1998). In the Central Graben, as extension continues, the rift axis becomes progressively more distant from the arc magmatic flux and can undergo magmatic extension (Gribble *et al.* 1998) and contamination by assimilation of rifted arc crust. As shown by Gribble *et al.* (1998), the distance between the axis of extension and the zone of sub-arc mantle downwelling is sufficient to allow the establishment of mantle upwelling and generate a MORB-like decompression melting system although slab signals are still detectable in the lavas.

In general, a subducted slab with old oceanic crust, oceanic sediment, and fluids that are returned to the mantle in subduction zones is

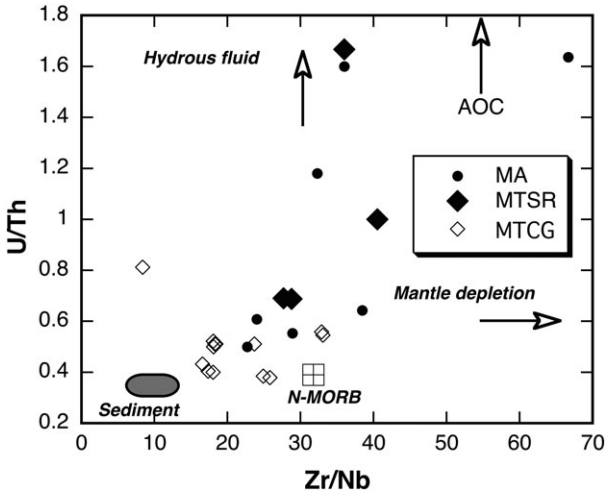

Fig. 11 U/Th vs Zr/Nb diagram after Stern *et al.* (2006) for samples from the Mariana Arc and the Mariana Trough. Composition of MORB from Sun and McDonough (1989), composition of sediment from Elliott *et al.* (1997). AOC, altered oceanic crustal material (Staudigel *et al.* 1996; Hochstaedter *et al.* 2001). Symbols are the same as those in Fig. 2.

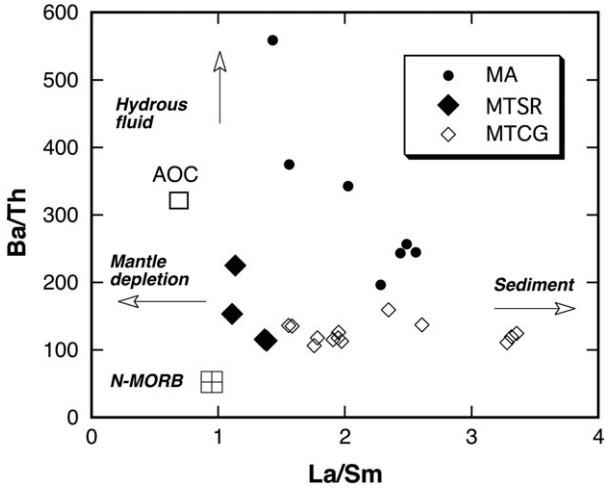

Fig. 10 Ba/Th vs La/Sm diagram modified after Elliott (2003) for samples from the Mariana Arc and the Mariana Trough. Composition of MORB from Sun and McDonough (1989). AOC, altered oceanic crustal material (Staudigel *et al.* 1996, Hochstaedter *et al.* 2001). Symbols are the same as those in Fig. 2.

characterized by radiogenic He and atmosphere-like Ne, Ar, Kr, and Xe isotopic compositions (e.g. Honda *et al.* 1993b; Bach & Niedermann 1998). The atmospheric noble gases are largely removed during subduction and are not mixed back into Earth's mantle (e.g. Staudacher & Allègre 1988; Moreira *et al.* 2003; Kendrick *et al.* 2011). Excesses in ^{129}Xe for the Mariana Trough samples in this study and in previous studies by Sano *et al.* (1998) and Ikeda *et al.* (1998) show that the mantle wedge is the principal source of volatiles where circumstances limit the amount of atmosphere-derived contributions (Hilton *et al.* 2002). Most Mariana Trough samples plot close to the MORB correlation line in the three-neon isotope systematics (Fig. 7). As mentioned before, this indicates binary mixing between atmospheric and mantle Ne. The mantle neon is a mixture of solar Ne (high ^{20}Ne/^{22}Ne $\approx$ 13) and nucleogenic Ne (high ^{21}Ne/^{22}Ne) in various proportions. Honda *et al.* (1993a) proposed that He and Ne isotopes are coupled and reflect addition of radiogenic ^{4}He and nucleogenic ^{21}Ne, produced throughout Earth history to primordial He and Ne captured at the time of planetary accretion (solar-neon hypothesis). Hilton *et al.* (2002) suggested that the Mariana Trough samples with MORB-like ^{3}He/^{4}He ratios substantiate the solar-neon hypothesis and indicate negligible input of He and Ne from any reservoir other than the mantle wedge. Bach and Niedermann (1998) recorded abundances of heavy noble gases with water contents and Ba/Nb ratios indicating subduction zone recycling of volatiles in Lau Basin samples. Hilton *et al.* (1993, 2002 suggested an alternative explanation, whereby low ^{40}Ar/^{36}Ar ratios in BABB indicate shallow-level contamination of arc-rifted crust during ageing and modification by hydrothermal alteration, causing an increase in radiogenic ^{4}He concentration and decrease in ^{4}He/^{40}Ar* and ^{40}Ar/^{36}Ar ratios.

^{3}He/^{4}He ratios of the Mariana Arc samples are MORB-like or slightly below MORB (Fig. 6), whereas Ne, Ar (except ^{40}Ar*), Kr, and Xe have isotopic compositions similar to atmosphere (Figs 7, 8 and Table 5). As already stated, high ^{4}He/^{20}Ne ratios (>12) for the Mariana Arc samples suggest that they are contaminated by the atmosphere, including seawater. Bach and Niedermann (1998) proposed that the atmospheric noble gases come from the subducting oceanic crust and are not due to shallow contamination with air dissolved in seawater or assimilation of old crust. Furthermore, Bach and Niedermann (1998) proposed that variations of ^{3}He/^{4}He changing from MORB-like to atmosphere-like result from radiogenic ingrowth of ^{4}He in the mantle wedge after it was enriched by U and Th released from the downgoing slab. ^{3}He/^{4}He in the Mariana Arc samples decreases with increasing Ba/Nb (Fig. 12), suggesting the relationship between He isotopic compositions and the extent of slab-derived fluid fluxing of the mantle wedge, as discussed by Bach and Niedermann (1998).

In a ^{4}He/^{40}Ar* vs Ba/Nb diagram (Fig. 13), Mariana Arc samples have low ^{4}He/^{40}Ar* and high Ba/Nb ratios, suggesting a fluid contribution, primarily because Ar is more soluble than He in water (e.g. Ozima & Podosek 2002) and seawater contamination is ruled out based on high ^{4}He/^{20}Ne

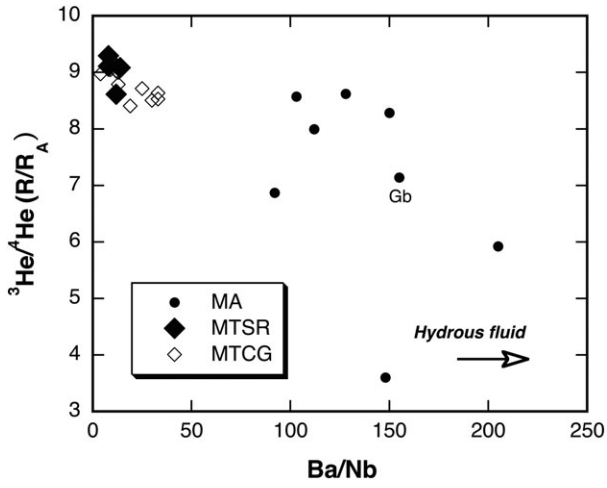

Fig. 12 ^{3}He/^{4}He (R/R$_A$, where R$_A$ = atmosphere value) vs Ba/Nb diagram for samples from the Mariana Arc and the Mariana Trough. Symbols are the same as those in Fig. 2.

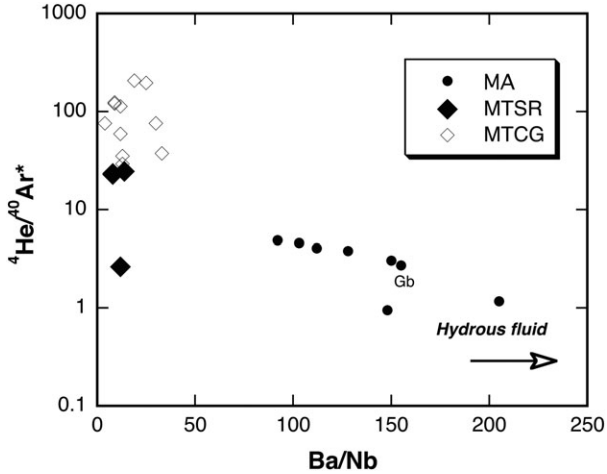

Fig. 13 ^{4}He/^{40}Ar* vs Ba/Nb diagram for samples from the Mariana Arc and the Mariana Trough. Symbols are the same as those in Fig. 2.

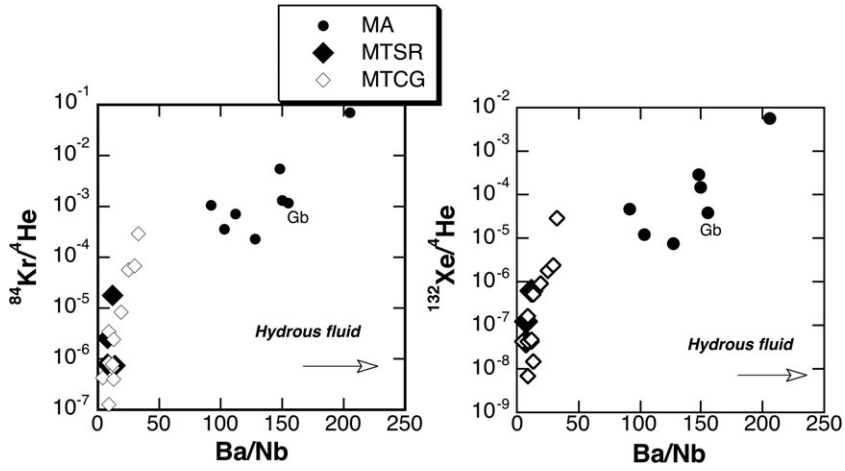

Fig. 14 $^{84}Kr/^{4}He$ vs Ba/Nb and $^{132}Xe/^{4}He$ vs Ba/Nb diagrams for samples from the Mariana Arc and the Mariana Trough. Symbols are the same as those in Fig. 2.

ratios. In contrast, samples from the Mariana Trough have high $^{4}He/^{40}Ar^{*}$ and low Ba/Nb ratios, indicating a melt derived from depleted mantle (Bach & Niedermann 1998), as He is more soluble than Ar in melts (Jambon *et al.* 1986; Ozima & Podosek 2002). The behavior of this relationship in the Mariana Arc samples is further assessed in Figure 14, with both $^{84}Kr/^{4}He$ and $^{132}Xe/^{4}He$ ratios correlating with fluid abundances (indicated by Ba/Nb ratios), as Kr and Xe are more soluble in water than He. The low $^{132}Xe/^{4}He$, $^{84}Kr/^{4}He$, and Ba/Nb ratios of the Mariana Trough basalts relative to the Mariana Arc rocks suggest that the generation of the former involved source depletion, as He is more soluble in melts than Xe and Kr.

Correlations of noble gas data in Figures 9, 13 and 14, as well as large ion lithophile elements (Figs 10, 11), indicate that heavy noble gases (Ar, Kr, and Xe) provide evidence for fluid fluxing in the mantle wedge.

CONCLUSIONS

The conclusions reached in this study can be summarized as follows:

1 The mantle source compositions beneath the Mariana Arc and the Mariana Trough show depletions in high field strength elements such as Nb relative to MORB.
2 The major element and Sr, Nd, He and Ne isotopic compositions of basalts from the Mariana Trough are geochemically indistinguishable from MORB.
3 Samples from the Mariana Arc, characterized by high Ba/Th, U/Th, $^{84}Kr/^{4}He$, and $^{132}Xe/^{4}He$, are explained by derivation from mantle that was affected by addition of fluid from the subducted slab.
4 Heavy noble gases (Ar, Kr, and Xe), as well as large ion lithophile elements, provide evidence for fluid fluxing of the mantle wedge.
5 Correlations of $^{3}He/^{4}He$ and $^{40}Ar/^{36}Ar$ in Mariana Trough samples are explained by mixing between a MORB-like mantle and atmosphere.
6 One sample from the Central Graben shows extreme enrichment in $^{20}Ne/^{22}Ne$ and $^{21}Ne/^{22}Ne$, suggesting incorporation of solar-type Ne in the magma source. This sample also contains excess ^{129}Xe, further suggesting primordial noble gases in the mantle source.
7 Correlations of variable La/Sm, Ba/Th, U/Th, and Zr/Nb among the Mariana Trough basalts indicate that the basalts contain contributions from both fluid and sediment melt components, with slab-derived fluid components dominating in the source of Spreading Ridge basalts, whereas sediment melt components, characterized by high La/Sm and low U/Th and Zr/Nb, dominate in Central Graben basalts.

ACKNOWLEDGEMENTS

Tha authors thank the scientific party, officers and crews of the 2001 R/V Melville of Scripps Institution of Oceanography the Cook 07 expedition, 2002 R/V Kairei of JAMSTEC KR02-01, and

2003 R/V Hakuho Maru of the University of Tokyo KH03-3 expedition. We wish to thank J. Ishioka, N. Nishi, and M. Sato for technical guidance of mass spectrometry at Niigata University. We thank Y. Motoyoshi, K. Shiraishi, and K. Seno for help with XRF analyses, and M. Otsuki for guidance and assistance of EPMA analyses. Preaparation of this paper was partly supported by the Ministry of Science, ICT and Planning (MSIP) of Korea. We thank AE A. Nichols for constructive comments and Mark Kendrick for his thoughtful criticism.

REFERENCES

ALLÈGRE C. J., STAUDACHER T. & SARDA P. 1986. Rare gas systematics: formation of the atmosphere, evolution and structure of the Earth's mantle. *Earth and Planetary Science Letters* **81**, 127–50.

BACH W. & NIEDERMANN S. 1998. Atmospheric noble gases in volcanic glasses from the southern Lau Basin: origin from the subducting slab? *Earth and Planetary Science Letters* **160**, 297–309.

BARNES J. D., SHARP Z. D. & FISCHER T. P. 2008. Chlorine isotope variations across the Izu-Bonin-Mariana arc. *Geology* **36**, 883–6.

BURNARD P. G., GRAHAM D. W. & FARLEY K. A. 2002. Mechanisms of magmatic gas loss along the Southeast Indian Ridge and the Amsterdam–St. Paul Plateau. *Earth and Planetary Science Letters* **203**, 131–48.

DEPAOLO D. J. 1988. *Neodymium isotope geochemistry*, Springer, Berlin Heidelberg New York.

ELLIOTT T. 2003. Tracers of the slab. *In* Eiler J. (ed.) *Inside the subduction factory, Geophysical Monograph* **138**, pp. 23–45, AGU, Washington DC.

ELLIOTT T., PLANK T., ZINDLER A., WHITE W. & BOURDON B. 1997. Element transport from slab to volcanic front at the Mariana arc. *Journal of Geophysical Research* **102**, 14991–5019.

FRETZDORFF S., LIVERMORE R. A., DEVEY C. W., LEAT P. T. & STOFFERS P. 2002. Petrogenesis of the back-arc East Scotia ridge, South Atlantic Ocean. *Journal of Petrology* **43**, 1435–67.

GASPARON M., HILTON D. R. & VARNE R. 1994. Crustal contamination processes traced by helium isotopes: Example from the Sunda arc, Indonesia. *Earth and Planetary Science Letters* **126**, 15–22.

GILL J. 1981. *Orogenic andesites and plate tectonics*, Springer, Berlin Heidelberg New York.

GRIBBLE R. F., STERN R. J., BLOOMER S. H., STUBEN D., O'HEARN T. & NEWMAN S. 1996. MORB mantle and subduction components interact to generate basalts in the southern Mariana Trough back-arc basin. *Geochimica et Cosmochimica Acta* **60**, 2153–66.

GRIBBLE R. F., STERN R. J., NEWMAN S., BLOOMER S. H. & O'HEARN T. 1998. Chemical and isotopic composition of lavas from the northern Mariana Trough: Implications for magmagenesis in back-arc basins. *Journal of Petrology* **39**, 125–54.

HANYU T., CLAGUE D. A., KANEOKA I., DUNAI T. J. & DAVIES G. R. 2005. Noble gas systematics of submarine alkalic lavas near the Hawaiian hotspot. *Chemical Geology* **214**, 135–55.

HAWKINS J. W. & MELCHIOR J. T. 1985. Petrology of Mariana Trough and Lau basin basalts. *Journal of Geophysical Research* **90**, 11431–68.

HAWKINS J. W., MACDOUGALL J. D. & VOLPE A. M. 1990. Petrology of the axial ridge of the Mariana Trough backarc spreading center. *Earth and Planetary Science Letters* **100**, 226–50.

HILTON D. R., FISCHER T. P. & MARTY B. 2002. Noble gases and volatile recycling at subduction zones. *In* Porcelli D., Ballentine C. J. and Wieler R. (eds.) *Noble gases in geochemistry and cosmochemistry, Reviews in Mineralogy and Geochemistry* **47**, pp. 319–70, Mineralogical Society of America, Washington D.C.

HILTON D. R., HAMMERSCHMIDT K., LOOCK G. & FRIEDRICHSEN H. 1993. Helium and argon isotope systematics of the central Lau Basin and Valu Fa Ridge: Evidence of crust/mantle interactions in a back-arc basin. *Geochimica et Cosmochimica Acta* **57**, 2819–41.

HOCHSTAEDTER A., GILL J., PETERS R., BROUGHTON P., HOLDEN P. & TAYLOR B. 2001. Across-arc geochemical trends in the Izu-Bonin arc: contributions from the subducting slab. *Geochemistry, Geophysics, Geosystems* **2**, , 2000GC000105.

HOLE M. J., SAUNDERS A. D., MARRINER G. F. & TARNEY J. 1984. Subduction of pelagic sediments; implications for the origin of Ce-anomalous basalts from the Mariana Islands. *Journal of the Geological Society, London* **141**, 453–72.

HONDA M., MCDOUGALL I. & PATTERSON D. B. 1993a. Solar noble gases in the Earth: The systematics of helium-neon isotopes in mantle derived samples. *Lithos* **30**, 257–65.

HONDA M., PATTERSON D. B., MCDOUGALL I. & FALLOON T. J. 1993b. Noble gases in submarine pillow basalt glasses from the Lau Basin: Detection of a solar component in backarc basin basalts. *Earth and Planetary Science Letters* **120**, 135–48.

IKEDA Y. 2006. Preparation of rock samples for Sr and Nd isotopic analysis at small scale petrochemical laboratory. *Journal of Hokkaido University of Education (Natural Sciences)* **57**, 33–9 (in Japanese with English abstract).

IKEDA Y., NAGAO K. & KAGAMI H. 2001. Effects of recycled materials involved in a mantle source beneath the southwest Japan arc region: Evidence from noble gas, Sr, and Nd isotopic systematics. *Chemical Geology* **175**, 509–22.

IKEDA Y., NAGAO K., STERN R. J., YUASA M. & NEWMAN S. 1998. Noble gases in pillow basalt glasses from the northern Mariana Trough back-arc basin. *Island Arc* **7**, 471–8.

IKEDA Y. & YUASA M. 1989. Volcanism in nascent back-arc basins behind the Shichito Ridge and adjacent areas in the Izu-Ogasawara arc, northwest Pacific: evidence for mixing between E-type MORB and island arc magmas at the initiation of back-arc rifting. *Contributions to Mineralogy and Petrology* **101**, 377–93.

IMAI N., TERASHIMA S., ITOH S. & ANDO A. 1995. 1994 compilacation of analytical data for minor and trace elements in seventeen GSJ geochemical reference samples, "Igneous rock series". *Geostandards Newsletter* **19**, 135–213.

JAMBON A., WEVER H. & BRAUN O. 1986. Solubility of He, Ne, Ar, Kr and Xe in a basalt melt in the range 1250-1600 °C. Geochemical implications. *Geochimica et Cosmochimica Acta* **50**, 401–8.

KANEOKA I. & TAKAOKA N. 1985. Noble-gas state in the earth's interior: Some constraints on the present state. *Chemical Geology* **52**, 75–95.

KELLEY K. A., PLANK T., NEWMAN S. *et al.* 2010. Mantle melting as a function of water content beneath the Mariana Arc. *Journal of Petrology* **51**, 1711–38.

KENDRICK M. A., SCAMBELLURI M., HONDA M. & PHILLIPS D. 2011. High abundances of noble gas and chlorine delivered to the mantle by serpentinite subduction. *Nature Geoscience* **4**, 807–12.

KURZ M. D. 1991. Noble gas isotopes in oceanic basalts: Controversial constraints on mantle models. *In* Heaman L. and Ludden J. N. (eds.) *Short Course Handbook 19 on Applications of Radiogenic Isotope Systems to Problems in Geology*, pp. 259–86, Mineralogical Association of Canada, Toronto.

LEMAITRE R. W. 1989. *A classification of igneous rocks and glossary of terms*, Blackwell Scientific, Oxford.

MACPHERSON C. G., HILTON D. R., MATTEY D. P. & SINTON J. M. 2000. Evidence for an ^{18}O-depleted mantle plume from contrasting $^{18}O/^{16}O$ ratios of back-arc lavas from the Manus Basin and Mariana Trough. *Earth and Planetary Science Letters* **176**, 171–83.

MARSKE J. P., PIETRUSZKA A. J., TRUSDELL F. A. & GARCIA M. O. 2011. Geochemistry of southern Pagan Island lavas, Mariana arc: the role of subduction zone processes. *Contributions to Mineralogy and Petrology* **162**, 231–52.

MARTINEZ F., FRYER P., BAKER N. A. & YAMAZAKI T. 1995. Evolution of back-arc rifting: Mariana Trough, 20°-24°N. *Journal of Geophysical Research* **100**, 3807–27.

MARTINEZ F. & TAYLOR B. 2003. Controls on back-arc crustal accretion: insights from the Lau, Manus and Mariana basins. *In* Larter D. and Leat P. T. (eds.) *Intra-oceanic subduction systems: tectonic and magmatic processes*, Geological Society of London, Special Publication **219**, pp. 19–54.

MATSUDA J., MATSUMOTO T., SUMINO H. *et al.* 2002. The $^{3}He/^{4}He$ ratio of the new internal He standard of Japan (HESJ). *Geochemical Journal* **36**, 191–5.

MOREIRA M., BLUSZTAJN J., CURTICE J., HART S., DICK H. & KURZ M. D. 2003. He and Ne isotopes in oceanic crust: implications for noble gas recycling in the mantle. *Earth and Planetary Science Letters* **216**, 635–43.

MOREIRA M. & SARDA P. 2000. Noble gas constraints on degassing processes. *Earth and Planetary Science Letters* **176**, 375–86.

MOTOYOSHI Y., ISHIZUKA H. & SHIRAISHI K. 1996. Quantitative chemical analyses of rocks with X-ray fluorescence analyzer: (2) Trace elements. *Nankyoku Shiryo (Antarctic Recor), National Institute of Polar Research* **40**, 53–63 (in Japanese with English abstract).

MOTOYOSHI Y. & SHIRAISHI K. 1995. Quantitative chemical analyses of rocks with X-ray fluorescence analyzer: (1) Major elements. *Nankyoku Shiryo (Antarctic Record), National Institute of Polar Research* **39**, 40–8 (in Japanese with English abstract).

OZIMA M. & PODOSEK F. A. 2002. *Noble Gas Geochemistry*, 2nd edn, Cambridge University Press, Cambridge, United Kingdom.

PEARCE J. A., BAKER P. E., HARVERY P. K. & LUFF I. W. 1995. Geochemical evidence for subduction fluxes, mantle melting and fractional crystallization beneath the South Sandwich island arc. *Journal of Petrology* **36**, 1073–109.

PEARCE J. A., STERN R. J., BLOOMER S. H. & FRYER P. 2005. Geochemical mapping of the Mariana arc-basin system: Implications for the nature and distribution of subduction components. *Geochemistry, Geophysics, Geosystems* **6**, Q07006. DOI:10.1029/2004GC000895.

PEATE D. W. & PEARCE J. A. 1998. Causes of spatial compositional variations in Mariana arc lavas: Trace element evidence. *The Island Arc* **7**, 479–95.

POREDA R. 1985. Helium-3 and deuterium in back-arc basalts: Lau Basin and the Mariana Trough. *Earth and Planetary Science Letters* **73**, 244–54.

SANO Y., NISHIO Y., GAMO T., JAMBON A. & MARTY B. 1998. Noble gas and carbon isotopes in Mariana Trough basalt glasses. *Applied Geochemistry* **13**, 441–9.

SANO Y., NAKAMURA Y., WAKITA H. & ISHII T. 1986. Light noble gases in basalt glasses from Mariana Trough. *Geochimica et Cosmochimica Acta* **50**, 2429–32.

SANO Y. & WAKITA H. 1985. Geographical distribution of $^{3}He/^{4}He$ ratios in Japan: Implications for arc tectonics and incipient magmatism. *Journal of Geophysical Research* **90**, 8729–41.

SARDA P. & GRAHAM D. W. 1990. Mid-ocean ridge popping rocks: implications for degassing at ridge crests. *Earth and Planetary Science Letters* **97**, 268–89.

SARDA P., STAUDACHER T. & ALLÈGRE C. J. 1988. Neon isotopes in submarine basalts. *Earth and Planetary Science Letters* **91**, 73–88.

SAUNDERS A. D., NORRY M. J. & TARNEY J. 1991. Fluid influence on the trace element compositions of subduction zone magmas. *Philosophical Transactions of the Royal Society of London, Series A* **335**, 377–92.

SENO K., ISHIZUKA H., MOTOYOSHI Y. & SHIRAISHI K. 2002. Quantitative chemical analyses of rocks with X-ray fluorescence analyzer: (3) Rare earth elements. *Nankyoku Shiryo (Antarctic Record), National Institute of Polar Research* **46**, 15–33 (in Japanese with English abstract).

SHAW A. M., HILTON D. R., MACPHERSON C. G. & SINTON J. M. 2001. Nucleogenic neon in high $^{3}He/^{4}He$ lavas from the Manus back-arc basin: a new perspective on He-Ne decoupling. *Earth and Planetary Science Letters* **194**, 53–66.

STAUDACHER T. & ALLÈGRE C. J. 1982. Terrestrial xenology. *Earth and Planetary Science Letters* **60**, 389–406.

STAUDACHER T. & ALLÈGRE C. J. 1988. Rycycling of oceanic crust and sediments: the noble gas subduction barrier. *Earth and Planetary Science Letters* **89**, 173–83.

STAUDACHER T., SARDA P., RICHARDSON S. H., ALLÈGRE C. J., SAGNA I. & DMITRIEV L. V. 1989. Noble gases in basalt glasses from a Mid-Atlantic Ridge topographic high at 14°N: Geodynamic consequences. *Earth and Planetary Science Letters* **96**, 119–33.

STAUDIGEL H., PLANK T., WHITE B. & SCHMINCKE H.-U. 1996. Geochemical fluxes during seafloor alteration of the basaltic upper oceanic crust: DSDP Sites 417 and 418. *In* Bebout G. E., Scholl D. W., Kirby S. H. and Platt J. P. (eds.) *Subduction top to bottom, Geophysical Monograph* **96**, pp. 19–38, AGU, Washington D.C.

STERN R. J., BLOOMER S. H., LIN P., ITO E. & MORRIS J. 1988. Shoshonitic magmas in nascent arcs: New evidence from submarine volcanoes in the northern Mariana. *Geology* **16**, 426–30.

STERN R. J., BLOOMER S. H., MARTINEZ F., YAMAZAKI T. & HARRISON T. M. 1996. The composition of back-arc basin lower crust and upper mantle in the Mariana Trough: A first report. *Island Arc* **5**, 354–72.

STERN R. J., FOUCH M. J. & KLEMPERER S. L. 2003. An overview of the Izu-Bonin-Mariana subduction factory. *In* Eiler J. (ed.) *Inside the subduction factory, Geophysical Monograph* **138**, pp. 175–222, AGU, Washington DC.

STERN R. J., JACKSON M. C., FRYER P. & ITO E. 1993. O, Sr, Nd and Pb isotopic composition of the Kasuga cross-chain in the Mariana Arc: A new perspective on the K-h relationship. *Earth and Planetary Science Letters* **119**, 459–75.

STERN R. J., KOHUT E., BLOOMER S. H., LEYBOURNE M., FOUCH M. & VERVOORT J. 2006. Subduction factory processes beneath the Guguan cross-chain, Mariana arc: no role for sediments, are serpentinites important? *Contributions to Mineralogy and Petrology* **151**, 202–21.

STERN R. J., LIN P., MORRIS J. D. *et al.* 1990. Enriched back-arc basin basalts from the northern Mariana Trough: implications for the magmatic evolution of back-arc basins. *Earth and Planetary Science Letters* **100**, 210–25.

STOLPER E. & NEWMAN S. 1994. The role of water in the petrogenesis of Mariana Trough magma. *Earth and Planetary Science Letters* **121**, 293–325.

SUN S.-S. & MCDONOUGH W. F. 1989. Chemical and isotopic systematics of oceanic basalts: implications for mantle composition and processes. *In* Saunders A. D. and Norry M. J. (eds.) *Magmatism in the Ocean Basins*. Geological Society of London, Special Publication **42**, pp. 313–45.

TAMURA Y., ISHIZUKA O., STERN R. J. *et al.* 2014. Mission Immiscible: Distinct subduction components generate two primary magmas at Pagan volcano, Mariana Arc. *Journal of Petrology* **55**, 63–101.

TANAKA T., TOGASHI S., KAMIOKA H. *et al.* 2000. JNdi-1; a neodymium isotopic reference in consistency with LaJolla neodymium. *Chemical Geology* **168**, 279–81.

TOLLSTRUP D. L. & GILL J. B. 2005. Hafnium systematics of the Mariana arc: Evidence for sediment melt and residual phases. *Geology* **33**, 737–40.

VOLPE A. M., MACDOUGALL J. D. & HAWKINS J. W. 1987. Mariana Trough basalts (MTB): Trace element and Sr-Nd isotopic evidence for mixing between MORB-like and arc-like melts. *Earth and Planetary Science Letters* **82**, 241–54.

WADE J. A., PLANK T., STERN R. J. *et al.* 2005. The May 2003 eruption of Anatahan volcano, Mariana Islands: Geochemical evolution of a silicic island-arc volcano. *Journal of Volcanology and Geothermal Research* **146**, 139–70.

WOODHEAD J., EGGINS S. & GAMBLE J. 1993. High field strength and transition element systematics in island arc and back-arc basin basalts: evidence for multi-phase melt extraction and a depleted mantle wedge. *Earth and Planetary Science Letters* **114**, 491–504.

WOODHEAD J., STERN R. J., PEARCE J., HERGT J. & VERVOORT J. 2012. Hf-Nd isotope variation in Mariana Trough basalts: The importance of "ambient mantle" in the interpretation of subduction zone magmas. *Geology* **40**, 539–42.

APPENDIX

Table A1 Representative compositions of olivines from samples for which noble gases were analyzed in olivines

Sample Analysis no.	SiO_2	TiO_2	Al_2O_3	FeO	MnO	MgO	CaO	Na_2O	K_2O	Cr_2O_3	V_2O_3	NiO	P_2O_5	Total	Si
D50–2-1: Basalt Mariana Arc (Central Islands Province)															
P-core174	37.48	0.02	0.04	21.91	0.37	37.04	0.28	0.02	0.02	0.01	0.00	0.00	0.02	97.20	1.004
P-rim175	37.45	0.01	0.04	22.64	0.49	37.35	0.29	0.04	0.00	0.08	0.04	0.13	0.00	98.56	0.995
D41–1-1: Gabbro Mariana Arc (Central Islands Province)															
core187	38.88	0.02	0.04	19.71	0.34	41.10	0.18	0.00	0.00	0.01	0.00	0.07	0.00	100.35	0.996
rim188	38.95	0.00	0.04	19.06	0.45	41.74	0.18	0.00	0.00	0.00	0.03	0.01	0.01	100.47	0.994
D31–1-1: Basalt Mariana Arc (Southern Seamount Province)															
P-core121	38.03	0.05	0.04	23.76	0.37	37.32	0.20	0.00	0.00	0.00	0.00	0.04	0.01	99.82	0.999
P-rim124	39.56	0.05	0.02	23.28	0.40	37.28	0.23	0.00	0.00	0.01	0.00	0.08	0.05	100.95	1.021
D31–2-3: Basalt Mariana Arc (Southern Seamount Province)															
P-core40	39.69	0.05	0.01	9.55	0.17	48.81	0.28	0.02	0.00	0.06	0.00	0.14	0.02	98.80	0.987
P-rim42	37.29	0.06	0.02	20.50	0.35	38.44	0.23	0.00	0.00	0.00	0.00	0.01	0.04	96.93	0.996
D14–1-2: Basalt Mariana Arc (Southern Seamount Province)															
P-core149	41.01	0.01	0.02	10.11	0.20	49.87	0.07	0.00	0.02	0.00	0.02	0.15	0.00	101.46	0.993
P-rim151	40.66	0.04	0.03	12.64	0.21	47.45	0.30	0.01	0.01	0.02	0.00	0.11	0.00	101.47	0.996
D65–2-2: Basalt Mariana Arc (Southern Seamount Province)															
P-core20	38.48	0.02	0.02	17.99	0.28	41.67	0.24	0.00	0.00	0.01	0.02	0.10	0.00	98.85	0.994
P-rim21	37.94	0.01	0.05	17.79	0.27	41.44	0.22	0.01	0.00	0.00	0.04	0.07	0.03	97.86	0.990
D8–301: Clinopyroxenite Mariana Arc (Forearc)															
I-45	38.63	0.00	0.04	18.70	0.40	40.52	0.16	0.02	0.05	0.00	0.00	0.17	0.04	98.73	1.002

P, phenocryst; I, interstitial mineral; Mg# = (Mg/Mg + Fe) × 100.

Table A1 *(Continued)*

Sample Analysis no.	Ti	Al	Fe	Mn	Mg	Ca	Na	K	Cr	V	Ni	P	Total cation oxygen = 4	Mg#
D50–2-1: Basalt Mariana Arc (Central Islands Province)														
P-core174	0.000	0.001	0.491	0.008	1.480	0.008	0.001	0.001	0.000	0.000	0.000	0.000	2.995	75
P-rim175	0.000	0.001	0.503	0.011	1.479	0.008	0.002	0.000	0.002	0.001	0.003	0.000	3.004	75
D41–1-1: Gabbro Mariana Arc (Central Islands Province)														
core187	0.000	0.001	0.422	0.007	1.569	0.005	0.000	0.000	0.000	0.000	0.001	0.001	3.004	79
rim188	0.000	0.001	0.407	0.010	1.588	0.005	0.000	0.000	0.000	0.001	0.000	0.000	3.005	80
D31–1-1: Basalt Mariana Arc (Southern Seamount Province)														
P-core121	0.001	0.001	0.522	0.008	1.461	0.006	0.000	0.000	0.000	0.000	0.001	0.000	2.999	74
P-rim124	0.001	0.001	0.502	0.009	1.434	0.006	0.000	0.000	0.000	0.000	0.002	0.001	2.977	74
D31–2-3: Basalt Mariana Arc (Southern Seamount Province)														
P-core40	0.001	0.000	0.199	0.004	1.809	0.008	0.001	0.000	0.001	0.000	0.003	0.000	3.011	90
P-rim42	0.001	0.001	0.458	0.008	1.530	0.007	0.000	0.000	0.000	0.000	0.000	0.001	3.001	77
D14–1-2: Basalt Mariana Arc (Southern Seamount Province)														
P-core149	0.000	0.000	0.205	0.004	1.799	0.002	0.000	0.001	0.000	0.000	0.003	0.000	3.007	90
P-rim151	0.001	0.001	0.259	0.004	1.732	0.008	0.000	0.000	0.000	0.000	0.002	0.000	3.003	87
D65–2-2: Basalt Mariana Arc (Southern Seamount Province)														
P-core20	0.000	0.001	0.389	0.006	1.605	0.007	0.000	0.000	0.000	0.000	0.002	0.000	3.005	81
P-rim21	0.000	0.001	0.388	0.006	1.613	0.006	0.001	0.000	0.000	0.001	0.001	0.001	3.008	81
D8–301: Clinopyroxenite Mariana Arc (Forearc)														
I-45	0.000	0.001	0.406	0.009	1.567	0.004	0.001	0.002	0.000	0.000	0.003	0.001	2.997	79

P, phenocryst; I, interstitial mineral; Mg# = (Mg/Mg + Fe) × 100.

Table A2 Representative compositions of clinopyroxenes from those samples for which noble gases were analyzed in clinopyroxenes

Sample Analysis no.	SiO_2	TiO_2	Al_2O_3	FeO	MnO	MgO	CaO	Na_2O	K_2O	Cr_2O_3	V_2O_3	NiO	P_2O_5	Total	Si
D8–301: Clinopyroxenite Mariana Arc (Forearc)															
core55	50.83	0.26	3.29	5.53	0.16	15.68	22.67	0.30	0.00	0.16	0.00	0.07	0.00	98.93	1.897
rim56	51.13	0.37	3.71	5.16	0.18	15.26	23.50	0.19	0.00	0.07	0.03	0.08	0.00	99.70	1.892

Mg# = (Mg/Mg + Fe) × 100.

Table A2 *(Continued)*

Sample Analysis no.	Ti	Al	Fe	Mn	Mg	Ca	Na	K	Cr	V	Ni	P	Total cation oxygen = 6	Mg#
D8–301: Clinopyroxenite Mariana Arc (Forearc)														
core55	0.007	0.144	0.172	0.005	0.872	0.906	0.021	0.000	0.005	0.000	0.002	0.000	4.032	83
rim56	0.010	0.162	0.160	0.006	0.842	0.932	0.014	0.000	0.002	0.001	0.003	0.000	4.022	84

Mg# = (Mg/Mg + Fe) × 100.